

RESEARCH ARTICLE

Neuroscience of Disease

Neuronal activity reorganization in motor cortex for successful locomotion after a lesion in the ventrolateral thalamus

 Irina N. Beloozerova^{1,2}

¹School of Biological Sciences, Georgia Institute of Technology, Atlanta, Georgia and ²Barrow Neurological Institute, St. Joseph's Hospital and Medical Center, Phoenix, Arizona

Abstract

Thalamic stroke leads to ataxia if the cerebellum-receiving ventrolateral thalamus (VL) is affected. The compensation mechanisms for this deficit are not well understood, particularly the roles that single neurons and specific neuronal subpopulations outside the thalamus play in recovery. The goal of this study was to clarify neuronal mechanisms of the motor cortex involved in mitigation of ataxia during locomotion when part of the VL is inactivated or lesioned. In freely ambulating cats, we recorded the activity of neurons in layer V of the motor cortex as the cats walked on a flat surface and horizontally placed ladder. We first reversibly inactivated 10% of the VL unilaterally using glutamatergic transmission antagonist CNQX and analyzed how the activity of motor cortex reorganized to support successful locomotion. We next lesioned 50%–75% of the VL bilaterally using kainic acid and analyzed how the activity of motor cortex reorganized when locomotion recovered. When a small part of the VL was inactivated, the discharge rates of motor cortex neurons decreased, but otherwise the activity was near normal, and the cats walked fairly well. Individual neurons retained their ability to respond to the demand for accuracy during ladder locomotion; however, most changed their response. When the VL was lesioned, the cat walked normally on the flat surface but was ataxic on the ladder for several days after lesion. When ladder locomotion normalized, neuronal discharge rates on the ladder were normal, and the shoulder-related group was preferentially active during the stride's swing phase.

NEW & NOTEWORTHY This is the first analysis of reorganization of the activity of single neurons and subpopulations of neurons related to the shoulder, elbow, or wrist, as well as fast- and slow-conducting pyramidal tract neurons in the motor cortex of animals walking before and after inactivation or lesion in the thalamus. The results offer unique insights into the mechanisms of spontaneous recovery after thalamic stroke, potentially providing guidance for new strategies to alleviate locomotor deficits after stroke.

cat; diaschisis; inactivation; limb control; pyramidal tract neuron

INTRODUCTION

Thalamic stroke leads to ataxia, i.e., incoordination of limb movements with dysmetria, if the cerebellum-receiving ventrolateral thalamus (VL) is affected (1–5). The recovery time ranges from 2 wk to over a year, and the accuracy of movements is the last capacity to recover (3). Preclinical animal studies showed that VL lesions impair skilled locomotion, compromise the accuracy of jumps, and increase the latency of reaching movements (6–12). Most of these deficits disappear in 1 mo. Both for humans and animals, the mechanisms of motor recovery after a VL

lesion are unclear, and this slows the development of new rehabilitation approaches for patients with thalamic ataxia.

Ataxia after a stroke involving the VL or during a transient ischemic attack (TIA or “ministroke”) affecting the VL is believed to be caused by a disruption of signal transmission in the cerebello-cortical pathway (e.g., Ref. 13). The VL connects the cerebellum to the motor cortex (e.g., Refs. 14–16), and the cerebellum is closely involved in the visuomotor coordination needed for guiding limbs to objects (17–22). The activity of neurons in the VL changes before voluntary limb movements (23–28) and during locomotion

Correspondence: I. N. Beloozerova (ibeloozerova3@gatech.edu).

Submitted 26 April 2021 / Revised 26 August 2021 / Accepted 30 October 2021



is modulated with the rhythm of strides and depends on the accuracy of stepping (29). During locomotion, the VL conveys two types of information from the cerebellum to the motor cortex—movement-related information received by the cerebellum from the locomotion-related network of the spinal cord (for review, see Refs. 22 and 30) and visual information about locations of objects in the environment received via the pons from the cortical visual areas of the “dorsal stream,” the “Where?” pathway (31). Understandably, disruption of the transmission of these signals to the motor cortex results in ataxia. In addition, the VL is more than a simple cerebellum-to-motor cortex relay, as motor, somatosensory, and visual information merge in the VL (29). The loss of this merged visuomotor information must also contribute to the ataxia.

The nervous mechanism of the recovery from ataxia caused by a lesion in the VL likely consists of two components—the recovery and compensation within the thalamus and reorganization of the activity of other brain centers involved in control of movements, starting with those that are directly connected with the VL. The motor cortex is one such center. It is the main target of the VL projection, and the input from the VL is the main subcortical input to the motor cortex. Lesions in the motor cortex severely compromise the accuracy of skilled movements, including the ability to successfully ambulate over complex terrain (32–39). Like that of the VL, the activity of the motor cortex during locomotion is modulated with the rhythm, and the intensity of this modulation depends on the complexity of the locomotor task (34, 40–61). The motor cortex has direct access to the spinal cord and reach connections with many other movement-controlling centers, including projections back to the VL. Thus, the motor cortex is well-positioned to compensate for a malfunction in the VL that leads to ataxia.

Many studies have investigated the changes in the global characteristics of motor cortex activity after a VL lesion, such as electro-encephalographic (EEG) and metabolic changes and reorganization of cortical “motor maps” (e.g., Refs. 62–70), or studied subcellular events (e.g., Refs. 71–73; see also Refs. 74 and 75). In thalamic stroke survivors and patients who have undergone thalamotomy aimed at the VL and nucleus ventralis interomedialis (Vim) for treatment of severe tremor, positron emission tomography (PET) has shown that metabolism in the cortex on the side of the thalamic lesion is significantly reduced after the lesion, and this reduction positively correlates with the severity of poststroke deficits and negative side effects of the thalamotomy (62–64). Functional magnetic resonance imaging (fMRI) has also shown that recovery after a subcortical stroke positively correlates with the restoration of normal activity in the motor cortex (65, 66, 76). Morphological examination of the motor cortex in cats with experimental lesions in the VL found multiple new synapses on proximal dendrites of pyramidal cells formed by axons from the somatosensory cortex (71) and an activity increase 2 wk after the lesion (72). A study of single-neuron discharges in the motor cortex conducted on anesthetized animals at different time points after a VL lesion showed that the firing rates of neurons were normal as soon as 1-wk postlesion, but the pattern of their activity and responses to somatosensory stimulation were altered (Ref. 77; see also Ref. 73). The contribution of individual neurons

and specific neuronal subpopulations of the motor cortex to recovery remain unclear.

Recently, while investigating how signals from the VL contribute to the formation of activity in the motor cortex in behaving cats, we found that during inactivation in the VL, the activity of the motor cortex layer V population was substantially reduced and the discharge of almost every neuron changed, although cats still walked essentially normally on the flat surface and stepped accurately on crosspieces of a horizontal ladder (78). We noted that the activity of different neurons often changed in opposite directions. Layer V is the output layer of the cortex, with neurons sending axons to many subcortical movement-related centers and the spinal cord. We hypothesized that the opposing changes in the activity of the neurons may compensate each other’s effects on the projection targets and thereby assist in preserving the locomotor function. We also wondered whether the observed changes in the patterns of neuronal activity might explain successful locomotion despite a lesion in the VL. The present study was aimed at elucidating the single-neuron mechanisms of reorganization of motor cortex activity that allow successful locomotion during a temporary inactivation and after a permanent lesion in the VL.

METHODS

Experimental Strategy

We conducted experiments in cats because the activity of the motor cortex during locomotion in cats with intact thalamus has been described in great detail (e.g., Refs. 34, 40–45, 49–53, and 79). This description provided the necessary reference for this study. Two adult domestic cats (*Felis catus*) were purchased from a certified commercial class B dealer—a female (cat A, weight 2.7 kg) and a male (cat B, weight 4.0 kg). They were trained and surgically prepared for chronic experiments. The activity of the motor cortex during simple and accuracy-demanding locomotion in normal conditions was investigated, and the results were published by Beloozerova et al. (80) for cat A and Beloozerova and co-workers (50, 78, 81) for both cats. Furthermore, the forelimb-related area of the VL was also investigated in both cats. This included a detailed description of somatosensory receptive fields (RFs), afferent connections of the area with the cerebellum and basal ganglia, projections of the area to the motor cortex, and a detailed characterization of neurons’ activity during simple and accuracy-requiring locomotion. These data were published by Marlinski et al. (29).

In the present study, we first analyzed how the locomotion-related activity of motor cortex neurons reorganizes during a short-lasting inactivation of a part of the VL that functionally models a TIA or “ministroke.” To do this, we inactivated for 2–4 h 10% of the VL on the same side of the brain as the recorded motor cortex by blocking excitatory inputs to VL neurons with a glutamatergic α -amino-3-hydroxy-5-methyl-4-isoxazolepropionic acid (AMPA) receptor antagonist 6-cyano-7-nitroquinoxaline-2,3-dione (CNQX) (82, 83), and observed the effect on the activity of motor cortex neurons. We recorded single-neuron activity in the motor cortex before and after VL inactivation and compared it for two locomotion tasks—simple locomotion on a flat surface and accurate stepping on

crosspieces of a horizontal ladder. Our earlier results showed that during such inactivation in the VL, the cats were still able to walk essentially normally both on the flat surface and the horizontal ladder (78), and we wondered how the activity of the motor cortex reorganizes to make this possible.

Next, in one of the cats (cat A), we analyzed how the locomotion-related activity of motor cortex neurons reorganizes after a permanent lesion of a larger part of the VL. To induce the lesion, we bilaterally injected kainic acid (KA) into the VL. KA is a direct agonist of the glutamate kainate receptors, and in high concentrations, it produces excitotoxic lesion of neurons while sparing passing fibers (8, 84, 85). We then recorded the activity of motor cortex neurons during flat surface and ladder locomotion for 1 mo after the lesion, and compared this to the activity of a group of neurons recorded from neighboring microelectrode tracks before the lesion.

To gain a more detailed insight into how the motor cortex may assist locomotion while the VL is malfunctioning, we investigated the activity of several neuronal subpopulations of the motor cortex. First, we used the known correspondence between the location of the somatosensory RF of a neuron and the part of the body the activity of this neuron influences (86–89) to compare responses of neurons related to different segments of the forelimb (the shoulder, elbow, and wrist/paw) to inactivation or lesion in the VL. We then characterized limb segment-related contributions of these neuronal groups to the maintenance of effective locomotion during a malfunction in the VL. Second, we used antidromic identification of pyramidal tract projecting neurons with fast- and slow-conducting axons (both cats) and neurons projecting to the red nucleus (cat A), a major midbrain motor center, to determine how these efferent subpopulations alter their signals to the downstream motor center and the spinal cord when the VL is temporarily inactivated or lesioned. The activity of efferent neurons shows the signals that the motor cortex sends out to ensure the success of locomotion behavior.

The part of this study that investigated reorganization in the motor cortex in response to reversible inactivation of a part of the VL with CNQX utilized the same data set as used by Beloozerova and Marlinski (78). The methods of surgical preparation, recording techniques, and data analyses have been described previously (29, 78, 90) and are only briefly reported here. The experimental protocol was in compliance with NIH guidelines for the care and use of animals in research, and was approved by the Barrow Neurological Institute Animal Care and Use Committee.

Animal Housing and Monitoring

Cats were housed in individual cages in all-female or all-male cat rooms. Environmental enrichment was provided in a separate cat enrichment room to which each cat had access for several hours twice a week. Cats were monitored daily by vivarium staff, weighed twice a week, and regularly attended by a licensed veterinarian; all the cats' health checks were conducted as required. Decisions regarding humane endpoints were at the discretion of the director of the vivarium, Dr. Martin.

Locomotion Tasks

We used two locomotion tasks: locomotion on a flat surface and locomotion on crosspieces of a horizontal ladder

(Fig. 1A). Locomotion on the flat surface can be accomplished without the VL or motor cortex, whereas accurate stepping on the ladder relies on participation of the thalamo-cortical network (11, 12, 32–35, 37–39, 91). Testing during these two tasks allowed us to compare how the motor cortex reorganizes after a lesion in the VL to participate in a task for which its function is essential, as opposed to a task for which it is not, thereby revealing the component of the reorganization that is essential for motor cortex-dependent function.

We used positive reinforcement with food to adapt cats to the experimental situation and to engage them in locomotion (92, 93). Cats walked in an experimental chamber, a rectangular enclosure with two parallel corridors (Fig. 1A). Each corridor was 2.5 m × 0.3 m. The surface of one corridor was flat, whereas the other corridor contained a horizontal ladder. The centers of the crosspieces on the ladder were spaced 25 cm apart, which is approximately half of a cat's average stride length during self-paced locomotion in the chamber with a flat floor (34, 80). The crosspieces had flat tops that were 5 cm wide. This slightly exceeded the 3 cm diameter support area of the cat paw (e.g., Ref. 94), so that the cats had full foot support on the crosspiece. Cats passed sequentially and repeatedly through the two corridors of the chamber, occasionally changing direction from clockwise to counterclockwise. After each round, cat received food in a feeding dish located in one of the chamber's corners. Cats were accustomed to wearing a cotton jacket, a light backpack with electrical connectors, and a sock with a small metal plate on the sole of the paw to record paw contact with the floor.

Recording and Analyzing Locomotor Behavior

A detailed analysis of the effects of inactivation and lesion in the VL on the biomechanics of locomotion was outside the scope of this study. Only general assessments sufficient to characterize overall performance were conducted. Each cat's passage through the beginning and end of each corridor was recorded using infrared photodiodes mounted in the walls of the chamber. The time to complete the passage was noted. The durations of the swing and stance phases of the stride were determined using the step-mark signal. To obtain this signal, the floor in the chamber and the crosspieces of the ladder were covered with electrically conductive rubberized material, and the cats were trained to wear an electro-isolative instrumented sock made of thin rubber. An electro-mechanical sensor was placed under the paw on the outside of the sock (e.g., Refs. 34, 43, 80, 90). We refer to the full movement cycle of one limb during locomotion (from beginning of swing to beginning of next swing of the same limb) as a step cycle or stride, and use these terms interchangeably. The stride duty factor was defined as the relative duration of the stance phase within the stride; it characterized the temporal structure of the stride. The effects of the testing condition (normal vs. CNQX in the VL and normal vs. KA in the VL) on the parameters of strides were tested using Student's two-tailed *t* test. The overall motor behavior of the animal was visually assessed and evaluated for any abnormalities. In selected experiments, the locomotor performance of the cat in the experimental chamber was videotaped.

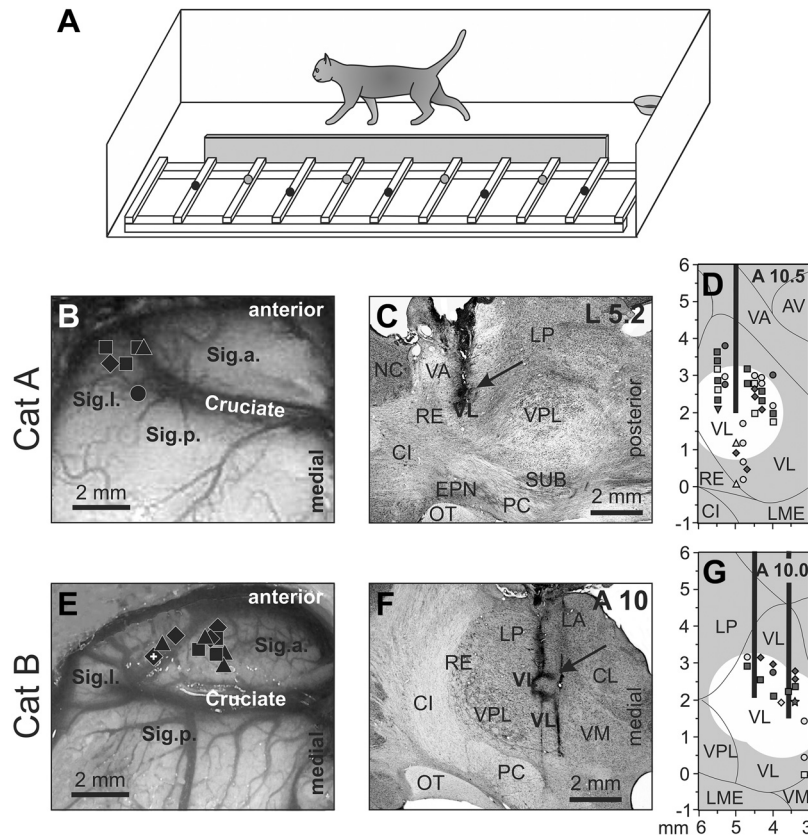


Figure 1. Locomotion tasks and reconstruction of recording sites in the motor cortex and injection sites in the ventrolateral thalamus (VL). A: the walking chamber was divided into two corridors. In one corridor, the floor was flat; the other corridor contained a horizontal ladder. Black circles on the crosspieces of the ladder schematically show placements of the right forelimb paw, whereas gray circles show those of the left forepaw. Sites of recording in the fore-limb representation of the left motor cortex of cat A (B) and cat B (E). Microelectrode entry points into the cortex are shown as symbols of different shapes. h, penetrations where the majority of neurons had receptive fields (RFs) on the shoulder, arm, and/or forearm but not the wrist or paw; ^, penetrations where most neurons had RFs on the wrist and/or paw. Overlapping symbols designate penetrations in which different neurons had RFs on different segments of the forelimb. A circle in B shows a penetration in which only neurons without a somatosensory RF were recorded (two neurons). In E, the microelectrode track where neurons were recorded—the activity of which is shown in Figs. 3 and 6—is indicated by a white cross. C, D, F, G: sites of recording and injection in the VL. Parasagittal (C) and frontal (F) sections of the thalamus of cats A and B, respectively. Cresyl violet stain. Arrows point to electrolytic lesion marks. D and G: reconstruction of areas of 6-cyano-7-nitroquinoxaline-2,3-dione (CNQX) inactivation in cat A (D) and cat B (G). These are modified fragments from Fig. 2D from Ref. 29. Vertical black bars schematically represent injection cannulas. White circles highlight approximate areas affected by CNQX. Symbols indicate the positions of VL neurons whose activity was described by Marlinski et al. (29). Squares show neurons with somatosensory RFs on the shoulder; dia-monds show cells that were activated by movements in the elbow; up-facing triangles indicate neurons with RFs on the wrist or paw; down-facing triangle shows a neuron whose RF encompassed the entire forelimb; and circles indicate neurons without somatosensory RFs and those where the RFs were not identified. Filled symbols represent neurons with axon projecting to the motor cortex; open symbols represent neurons whose axonal projections were not identified. AV, nucleus anteroventralis thalami; CI, capsula interna; CL, nucleus centralis lateralis; Cruciate, sulcus cruciatus; EPN, nucleus entopeduncularis; LA, nucleus lateralis anterior; LME, lamina medullaris externa thalami; LP, nucleus lateralis posterior; NC, nucleus caudatus; OT, optic tract; PC, pedunculus cerebri; RE, nucleus reticularis thalami; Sig.a., gyrus sigmoideus anterior; Sig.l., gyrus sigmoideus lateral; Sig.p., gyrus sigmoideus posterior; SUB, nucleus subthalamicus; VA, nucleus ventralis anterior; VL, nucleus ventralis lateralis; VM, nucleus medialis; VPL, nucleus ventralis posterolateralis.

These video recordings were visually examined and evaluated by two independent investigators who, while blind to the experimental condition, classified each trial as being obtained before or after a pharmacological intervention in the VL.

In cat A, in which selected muscles were implanted with electromyographic (EMG) electrodes, the EMG activity during locomotion was compared before and after the KA lesion. The effect of the reversible inactivation of part of the VL with CNQX on EMG activity during locomotion was not studied.

Surgical Procedures

Surgery was performed under isoflurane anesthesia using aseptic procedures. The skin and fascia were retracted from

the dorsal surface of the skull. At 10 points around the circumference of the skull, stainless-steel screws were implanted. The screw heads were then embedded into a plastic cast that formed a circular base. This base was later used for fixation of electrical connectors, an electrode micro-drive, and a preamplifier, as well as to rigidly hold the cat's head while searching for neurons.

On the left side of the head, the dorsal surfaces of the anterior and lateral sigmoid gyri and the rostral part of the posterior sigmoid gyrus were exposed by removal of 0.6 cm^2 of bone and dura mater. The region of the left motor cortex was visually identified based on surface features and photographed (Fig. 1, B and E). The exposure was covered with a 1-mm thick acrylic plate. The plate was pre-perforated with

holes of 0.36 mm in diameter spaced at 0.5 mm; the holes were filled with bone wax and Vaseline mixture. The plate was fixed to the surrounding bone using orthodontic resin (Dentsply Caulk, Milford, DE).

To identify axonal projections of motor cortical neurons to the pyramidal tract, two 26-gauge hypodermic guide tubes fitted with stainless-steel wires were implanted 7 mm above the left medullary pyramidal tract, placed 1 mm apart in the rostro-caudal direction. Later, in the awake cat, a 200- μ m platinum-iridium in Teflon insulation wire was inserted into the medullary pyramid under physiological guidance (90) to serve as a stimulation electrode for identification of axonal projections of motor cortical neurons to the pyramidal tract. In cat A, an arrangement of seven 28-gauge hypodermic guide tubes was implanted 8 mm above the left red nucleus. Later, in the awake cat, a 125- μ m platinum-iridium wire was placed in the red nucleus after its location was verified using single-neuron recording procedures (95). This wire served as a stimulation electrode for the identification of axonal projections of motor cortical neurons to the red nucleus.

An arrangement of 7 (cat A) or 19 (cat B) 28-gauge hypodermic guide tubes fitted with stainless steel wires was implanted bilaterally above the VL. The tip of the arrangement was placed at the vertical Horsley and Clarke coordinate V β 7.0, which is 2–5 mm above the top of the VL. Recordings of neuronal activity in the VL, inactivation of part of the VL with CNQX, and lesions in the VL with KA were accomplished via these tubes.

In cat A, the right and left *m. triceps* (elbow extensor) and the right and left *m. vastus lateralis* (knee extensor) were implanted with EMG electrodes using conventional methods. Immediately after the surgery and 12 h thereafter, an analgesic buprenorphine was administered subcutaneously.

Recording and Identifying Neurons in the Motor Cortex

Several days after the surgery, the cat was placed on a table equipped with a comforting pad and encouraged to take a “sphinx” posture. After the cat rested in this posture for several minutes, the base attached to the skull during surgery was fastened to an external frame so that the resting position of the head was approximated. This procedure minimizes stress on the neck while the head is immobilized. After a few training sessions, both cats sat quietly with their head restrained. They did not seem to be disturbed by the restraint and frequently fell asleep while sitting.

Extracellular recordings of single-neuron activity were obtained from the motor cortex forelimb representation area in the anterior and lateral sigmoid gyri (Fig. 1, B and E). This area of the cortex is considered the forelimb-related motor cortex, based on a considerable body of data obtained by means of inactivation, stimulation, and recording techniques (34, 79, 80, 96–100). Because the specific location of the area varies slightly among subjects, its position in each cat was identified using multiple-unit RF mapping procedures before recording experiments were initiated.

Tungsten varnish-insulated microelectrodes (120 mm outer diameter, impedance 1–3 MX at 1,000 Hz; FHC Inc., Bowdoin, ME) were used to record the activity of single neurons. A custom-made light-weight (2.5 g) manual single-axis micromanipulator chronically mounted on the cat’s head

was used to advance the microelectrode. Signals from the microelectrode were preamplified with a miniature, custom-made preamplifier on the cat’s head, and then further amplified and filtered (0.3–10 kHz band pass) with the CyberAmp 380 (Axon Instruments). After amplification, signals were digitized with a sampling frequency of 30 kHz and recorded using the computerized data acquisition and analysis package Power-1401/Spike-2 (Cambridge Electronic Design, Cambridge, UK). The Power-1401/Spike-2 waveform-matching algorithm was initially used to identify and isolate the spikes of single neurons. Only well-isolated neurons with stable spike shape were used for further analyses (e.g., Figs. 3 and 6).

The somatic receptive fields of the neurons were examined in animals resting with their head restrained. Somatosensory stimulation was produced by lightly stroking fur, palpation of the muscle bellies and tendons, and passive movements around limb joints. Receptive field size was determined by measuring the entire area from which action potentials could be elicited. Neurons responsive to passive movements were assessed for directional preference.

Neurons with axons descending within the pyramidal tract—pyramidal tract projection neurons (PTNs)—were identified based on their antidromic responses to electrical stimulation of the tract at the medulla level using the test for collision of spontaneous and evoked spikes (101, 102; see also, Refs. 50 and 78). The pyramidal tract was electrically stimulated with single rectangular pulses of 0.5 mA current with a duration of 0.2 ms. The distance between the stimulation electrode in the medullary pyramidal tract and recording sites in the peri-cruciate cortex was estimated at 51.5 mm, which included the curvature of the pathway. Neurons were classified as fast- or slow-conducting based on the criteria of Takahashi (103), i.e., neurons with an axonal conduction velocity of 21 m/s or higher were considered to be fast-conducting, whereas those with conduction velocities below this were considered to be slow-conducting.

In cat A, a number of PTNs sent an axonal collateral to the red nucleus in the midbrain, and three non-PTNs were identified as projecting axons to the red nucleus (cortico-rubral neurons). These projections were identified based on neurons’ antidromic responses to electrical stimulation of the red nucleus. The distance between the stimulation electrodes in the red nucleus and recording sites in the peri-cruciate cortex was estimated to be 40 mm. The identification of the red nucleus and the activity of its neurons in this and other cats while cats performed postural corrections during a separate set of experiments is reported by Zelenin et al. (95).

Each recorded neuron was tested for antidromic activation before, during, and after every locomotion test. Stimulating pulses typically did not evoke any visible motor responses, and they never produced any signs of discomfort or distress in the cats. All recordings were obtained from cortical layer V, which was identified by the presence of neurons with axons descending within the pyramidal tract.

Identification of the Forelimb-Related Area in the VL

We recognized the divisions of the thalamic ventrolateral nuclear complex in accordance with the nuclear delineation of the cat brain atlas of Reinoso-Suarez (104). We denoted

the posterior division of the complex as the ventral lateral nucleus (VL) and the anterior division of the complex as the ventral anterior nucleus (VA). These divisions in the cat are analogous to the posterior and anterior divisions of the primate ventral lateral nucleus, termed VLp and VLa, respectively.

During chronic experiments, the VL was identified using stereotaxic coordinates, responses of neurons to somatosensory stimulation, and antidromic responses to electrical stimulation of the motor cortex as described in detail by Marlinski et al. (29). The location of the VL was then verified by postmortem histological examination (Fig. 1, C and F). It showed that in cat A, the implanted guide tube arrangement targeted the anterior portion of the VL, whereas in cat B, the arrangement was aimed at the central part of the VL (29).

The forelimb-related area in the VL was identified by examining the somatosensory RFs of the neurons. As described by Marlinski et al. (29), 75% of neurons in the VL area, which we reversibly inactivated and then lesioned in cat A in the course of the experiments described here, had a somatosensory RF on the contralateral forelimb or neck and only 3.6% had RFs on the contralateral hindlimb. In Fig. 1, D and G, VL neurons with somatosensory RFs on different segments of the forelimb are shown by symbols of different shapes. There was no somatotopy within this area, as neurons responding to stimulation of different parts of the forelimb were distributed throughout this area without any clear clusters of shoulder-, elbow-, or wrist/paw-related cells.

The fact that the area of the VL that we inactivated and then lesioned in the experiments described here was primarily the cerebellum-receiving subdivision of the ventrolateral thalamus was confirmed by tracing afferent connections of the area done as a part of the previous study (29). As detailed there, after injection of horseradish peroxidase-conjugated wheat germ agglutinin (WGA-HRP) in the VL of cat A, numerous retrogradely labeled neurons were found in the anterior half of the lateral (dentate) nucleus of the contralateral cerebellum and in the anterior interposed nucleus of the contralateral cerebellum (Fig. 3A in Ref. 29). Ipsilaterally, labeled cells were found in the lateral half of the entopeduncular nucleus, which is the feline analog of the primate globus pallidus pars interna. In cat B, fluorescent beads were used for the tracing. In this cat, retrogradely labeled cells were found contralaterally throughout the rostro-caudal extent of the dentate and posterior interposed nuclei of the cerebellum, and several cells were found in the anterior interposed and fastigial nuclei of the cerebellum (Figs. 3 and 4 in Ref. 29). The entopeduncular nucleus did not have labeled cells in this cat.

The activity of the VL neurons during flat surface and ladder locomotion was recorded in these cats during the preceding separate set of experiments and reported by Marlinski et al. (29). The activity was step-cycle modulated and depended on whether locomotion required visuomotor coordination and accuracy of steps (on the ladder) or not (on the flat surface).

Experiments with Reversible Inactivation of Part of the VL

Reversible inactivation of part of the VL was achieved by a microinjection of a glutamatergic AMPA/kainate receptor

antagonist CNQX (82, 83) in the VL. Many sources providing input to the thalamus, including the cerebellum (105), sensorimotor cortex (106), and spinal cord (107, 108), use glutamate as a neurotransmitter and excite thalamic neurons. We blocked these excitatory inputs to the VL neurons, dramatically reducing their activity. Although this was not an ischemic event, the reduction of the VL activity allowed us to investigate how the motor cortex reorganizes in response to a temporary lost signal from the VL.

Recording protocol.

On each experimental day, 1–3 motor cortical neurons were identified by their somatosensory RF, projection of the axon, and axonal conduction velocity. Their activity during flat surface and ladder locomotion was first recorded in “normal” conditions when two or three data sets were collected 1 h apart, each consisting of the cat completing 30 rounds around the chamber. Between the recordings, the cat sat for 45–50 min on a comforting pad with its head restrained. If the activity of at least one neuron during locomotion—as determined by the analyses of the rasters and histograms of the neuron(s) stride-related discharges—in two consequent datasets was similar and the quality of the recording remained good, CNQX was injected into the left VL (see Injection of CNQX section below). Immediately after the injection, and then 40–60 min and 2, 3, and 4 h thereafter, neurons’ activity was recorded during 30 rounds of walking around the chamber. Similarly to the preinactivation data collection, recordings after the inactivation were separated by 45–50 min intervals when the cat sat with the head restrained.

Injection of CNQX.

CNQX was obtained from Sigma-Aldrich (CAS No. 115066-14-3). In each experiment, 1.0–2.5 μ L of 4.5 mM (cat A) or 1.5–2 μ L of 7.4 mM (cat B) CNQX dissolved in 0.9% NaCl solution was injected through a 35-gauge needle of a 10-mL Hamilton micro-syringe. The needle was lowered into the VL through an implanted guide tube (Fig. 1, D and G). The needle was connected to the syringe via a calibrated silicone tube. The CNQX was delivered in portions of 0.1 mL over a period of 10–15 min. Additional 5 min were allowed for diffusion of the substance before the needle was slowly withdrawn. The guide tube was then sealed with a fitting wire. In cat A, CNQX was injected in a single site of the left VL with coordinates A10.5, L5.0, and V \pm 2.0 (Fig. 1, C and D), whereas in cat B, CNQX was injected in various sites of the left VL within coordinates in the range of A10.0–10.5, L3.5–4.5, and V \pm 1.5 to \pm 2 (Fig. 1, F and G).

Verification of the effect of CNQX in the VL.

To verify the effect of CNQX on the activity of VL neurons and estimate the size of the affected area, in selected experiments, recordings were made from the VL sites located 720 mm and 1,080 mm away using 28-gauge guide tubes of the implanted arrangements, which were 360 mm in outer diameter. These recordings were taken during and immediately after the CNQX injection, as well as at all later times at which the activity in the cortex during locomotion was recorded. They showed that, with the volumes and concentrations of CNQX solutions used, a VL area of 2 mm³ in diameter was

inactivated for a period of 1.5–4 h, as neurons 0.72–1.08 mm away in either direction from the injection site were largely silent during this period (78). This estimate of the spread of CNQX is consistent with the estimates of drug diffusion in the brain obtained in the study of Myers (109). A volume of 2 mm³ represents 10% of the VL total volume, which is 20 mm³ in cats. Injections always resulted in a dramatic reduction of activity in neighboring VL areas and changes in the activity of motor cortical neurons (see RESULTS). That multiple subsequent CNQX injections were effective suggests that damage to the thalamic tissue resulting from the injections was small.

Experiment with Bilateral Lesions in the VL

Permanent bilateral lesions in the VL were generated in cat A by microinjections of kainic acid (KA). KA is a direct agonist of the glutamate kainate receptors, and in high concentrations, it produces an excitotoxic lesion, that is, death of neurons caused by their extreme excitation. Because glutamate receptors are present on the somatas of neurons but not axons, KA only lesions the neurons, affecting their somatas, but it does not damage passing fibers. Bilateral rather than unilateral lesions were induced to maximize the damage of the VL to motor cortex signaling.

Injection of KA.

Lesions in the VL were created in cat A immediately after completion of the experiments with reversible inactivation of the VL with CNQX. This was 3 mo after recordings in the motor cortex were initiated in this cat. KA was injected while the cat was under isoflurane anesthesia. A solution of KA (Sigma CAS No. 58002-62-3) in phosphate buffer at a concentration of 2 mg/mL was used for the injection. Injections were performed with the Precise Microinjection Unit Dagan PMI-200. KA was delivered via a glass tube (120 mm outer diameter, 50 mm inner diameter) that directly led from the Microinjection Unit into the brain. On the left side of the brain, the injection tube was placed into the VL at coordinates A10.5, L5, and V \pm 2 using the most caudal cannula. KA solution in the amount of 510.5 nL was injected in 1.4 nL portions over a period of 15 min. Additional 10 min was allowed for the diffusion of the substance before the tube was slowly removed and the guide cannula sealed with a fitting wire. On the right side, the injection tube was placed into the VL 1 mm more caudally, at A9.5, and 0.5 mm more medially, at R4.5, and at the same vertical coordinate of V \pm 2 mm. KA solution in the amount of 480 nL was injected in a similar manner as on the left side. The time between injections was 40 min.

After discontinuation of the anesthesia, the cat was closely monitored for 7 h and every day thereafter for 43 days. The overall behavior was assessed, and starting on the second day after the injections, locomotion on the flat surface and the ladder was tested. Recordings of the activity of motor cortical neurons were started on the second day after the injections and proceeded almost daily for the next 34 days. The group activities of neurons in layer V of the motor cortex recorded in this cat before and after the KA injections were compared.

In vivo verification of the effect of KA in the VL.

We previously found that VL lesions render cats unable to walk on the ladder (11, 12). Therefore, we expected that in

normal conditions, VL inactivation with muscimol, a selective agonist for GABA receptors, would also lead to a deficit in ladder locomotion. In contrast, if the VL was already lesioned by KA, injection of muscimol would not result in any additional deficits, confirming the VL destruction. Thus, to assess the effectiveness of the lesion of the VL by KA, injections of muscimol were made in the VL 3–17 days before and 30–32 days after the KA lesions. Locomotion on the flat surface and the ladder was visually assessed and videotaped, and it was compared before and after muscimol injection (15 min and 1, 2, and 4 h after).

Muscimol (MP Biomedicals Inc. No. 195336) dissolved in 0.9% NaCl solution at a concentration of 2 mg/mL was used. In the left VL, 17 days before the KA injection (and two days before the start of experiments with CNQX), 1 mL of muscimol was injected at coordinates of A10.5, L5, and V \pm 2 through the most caudal cannula. These were the same coordinates at which KA was later injected. In the right VL, 1.1 mL of muscimol in the same concentration was injected at coordinates A9.5, R4.5, and V \pm 2.0 2 wk later, 3 days before the KA injection at the same coordinates. Both muscimol injections were done while the awake cat sat with its head restrained. A 5-mL Hamilton syringe connected to a needle inserted in the VL through an implanted cannula was used to make an injection. An injection was done over 5–10 min and additional 5 min were allowed for diffusion of the substance before the needle was slowly removed and the guide cannula sealed with a fitting wire. The effect of muscimol on neuronal activity in the VL was monitored by recording with microelectrodes positioned via neighboring cannulas.

Processing of Neuronal Activity

From the four or five strides that cats took along each corridor (Fig. 1A), two strides in the middle of each corridor were selected for the analyses. The strides were additionally selected so that their average duration during flat surface and ladder locomotion differed by no more than 10%. It was previously shown that the activity of only a minority of neurons in the motor cortex reflects the speed of locomotion (40, 43). Nevertheless, selecting strides of a similar duration minimized any potential differences in the activity of neurons because of the difference in the speed of locomotion in the two tasks. Each group of selected strides contained at least 15 strides.

During the data analysis, the onset of swing of the right forelimb was taken as the beginning of the step cycle. The step cycles were time normalized, and raster plots were created to visualize the discharge of the neuron over all selected cycles of a locomotor task (e.g., Fig. 3, B and D). The duration of each step cycle was divided into 20 equal bins, and a phase histogram of the discharge rate of a neuron in the cycle was generated and averaged over all selected cycles (e.g., Fig. 3, C and E). The phase histograms were smoothed by recalculating the value of each bin as follows: $F_n^0 = 0.25 F_{n-1} + 0.5 F_n + 0.25 F_{n+1}$, where F_n is the original value of a bin. The “depth” of modulation, dM, was calculated as $dM = (N_{\max} - N_{\min})/N \cdot 100\%$, where N_{\max} and N_{\min} are the numbers of spikes in the maximal and minimal histogram bins and N is the total number of spikes in the histogram. Neurons with $dM > 4\%$ were judged to be stride related. This

was based on an analysis of fluctuations in the activity of neurons in the resting animal (50, 110). The portion of the cycle in which the discharge rate exceeded the value of the minimal rate plus 25% of the difference between the maximal and minimal rates in the histogram was defined as a period of elevated firing (PEF, Fig. 3, C and E). PEFs were smoothed by removing all one-bin peaks and troughs. In neurons with a single PEF per cycle, the preferred phase (PrPh) of the activity was assessed using circular statistics (111–113).

The following parameters were calculated for each neuron: the mean discharge frequency, dM, number of PEFs, duration of PEF(s), and for neurons with a single PEF, the PrPh. For individual neurons, the difference in each activity parameter between locomotion in normal conditions and each data set after CNQX injection was determined. For the comparison of the discharge rate in different conditions, the Student's two-tailed *t* test was used. When comparing dMs, PrPhs, and durations of PEFs, differences equal to or greater than 2%, 10%, and 20%, respectively, were considered significant. These criteria were established based on the results of a bootstrapping analysis that compared differences in the parameters between various reshufflings of strides of the same locomotion condition (50, 110).

For populations of neurons, the following parameters were calculated and compared between conditions: the proportion of neurons at their PEF during different phases of the step cycle, the distribution of the average population discharge frequency over the step cycle, the range of coefficients of modulation, and the average widths of PEFs. The difference in each mean parameter of the population activity between conditions was tested using the Student's two-tailed *t* test. Unless otherwise noted, for all mean values, the standard deviation (SD) is given. When data were categorical, a nonparametric Mann–Whitney (U) test, Fisher's two-tailed test, or Z test for proportions was performed. The significance level for all tests was set at 0.05.

Histological Procedures

On the day of termination, the cats were deeply anesthetized with pentobarbital sodium, and reference electrolytic lesions were made in the areas of recording and stimulation. The cats were perfused with 4% paraformaldehyde solution, and the brains were harvested. Frozen brain sections of 40 μ m thickness were cut in the regions of recording and stimulating electrodes, as well as the sites of CNQX and KA injections. The tissue was stained for the Nissl substance with cresyl violet or thionine. The positions of the recording tracks in the cortex and injection sites in the VL were estimated in relation to the reference lesions. The positions of the stimulation electrodes in the medullar pyramids, and for cat A, in the red nucleus were verified. Further details of the histological procedures can be found in our previous publications (29, 95).

The areas of the thalamus lesioned following KA injections were determined by inspecting sections through the thalamus and estimating the borders of the lesions in relation to the surviving nuclei. To estimate the volume of the damaged

tissue, lesioned areas were traced using a custom plotting system that combined digital imaging with information derived from the microscope stage position.

RESULTS

Reorganization of Motor Cortex Activity during Temporary Inactivation of Part of the VL

Inactivation of 10% of the VL unilaterally had a very minor effect on locomotion behavior.

Although CNQX always silenced the injected VL area (78) and evoked substantial changes in the activity of motor cortical neurons, as described next, only very small abnormalities in locomotion behavior were observed, and only in cat A. This cat missed a ladder crosspiece a couple of times per day shortly after CNQX was injected into the VL on the first three experimental days. Otherwise, the cat behaved and moved normally on these and all other days when a part of the VL was inactivated with CNQX. No motor deficits were seen in cat B.

During trials immediately preceding injection of CNQX in the VL, cats walked around the chamber 12–40 times. From these trials, 20–120 strides were selected according to the criteria outlined in METHODS for the analyses of each locomotion task in normal conditions. Across cats and testing days, the stride duration was in the range of 550–850 ms, which corresponded to the locomotion speed of 0.6–0.9 m/s. Detailed characteristics of the strides under normal conditions are given in Fig. 2A for individual cats and pooled across cats in Table 1.

Blocks of postinjection trials were selected for the maximal effect of CNQX in the VL on the locomotion-related activity of each motor cortical neuron. These trials were either those immediately following the injection or recorded 30–45 or 60 min later.¹ During blocks of these trials, cats walked around the chamber 11–38 times. Between 15 and 107 strides were selected per data set for the analyses of each locomotion task during inactivation in the VL. Across cats and testing days, the stride duration was in the range of 660–730 ms, corresponding to a locomotion speed of 0.7–0.8 m/s (Fig. 2A, Table 1).

After a part of the VL was inactivated, cat A walked on the flat surface slightly slower (by 3.4%; $P < 0.05$, *t* test), and it walked with a similar pace on the ladder (Fig. 2A). Cat B walked slower than cat A overall during both tasks; however, it walked with a similar pace before and after inactivation of part of the VL during both tasks (Fig. 2A). The stride's duty factor, which characterizes the structure of the stride, was similar in both cats before and after inactivation of part of the VL during ladder locomotion, and in cat B, it was also similar during flat surface locomotion (Fig. 2A).

Neuronal sample.

The activity of 35 neurons from layer V of the motor cortex was recorded during locomotion before and after inactivation of part of the VL with CNQX. Eighteen neurons were recorded from 5 tracks throughout the anterior aspect of the lateral sigmoid gyrus in cat A (Fig. 1B), and 17 neurons were

¹Blocks of postinjection trials selected: immediately following the injection ($n = 13/15$ for flat surface/ladder locomotion), 30–45 min after the injection ($n = 16/18$ for flat surface/ladder locomotion), and 60 min after the injection ($n = 12/9$ for flat surface/ladder locomotion).

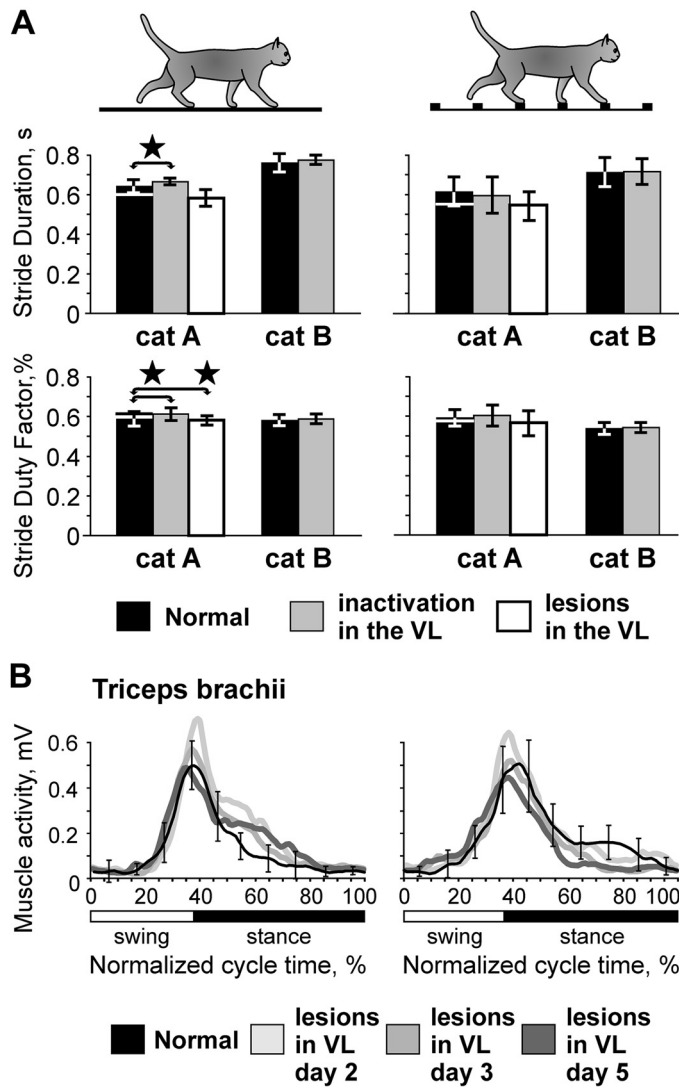


Figure 2. Characteristics of flat surface (left) and ladder (right) locomotion in normal conditions, after unilateral temporary inactivation in the ventrolateral thalamus (VL) with 6-cyano-7-nitroquinoxaline-2,3-dione (CNQX), and after bilateral permanent lesions in the VL with kainic acid (KA; cat A only). Silhouettes of cats indicate locomotor behavior. A: parameters of strides. Top: the average duration of the step cycle during flat surface and ladder locomotion; bottom: the stride duty factor (ratio of stance to step cycle duration). Black bars show normal condition data for experiments with temporary inactivation in the VL. For cat A, a white horizontal line at the top of each black bar shows the normal condition value taken for the experiment with lesions in the VL. Gray bars show data obtained after unilateral temporary inactivation of part of the VL with CNQX, and white bars show data obtained after bilateral KA-induced lesions in the VL (cat A only). Error bars show SDs. Stars indicate statistically significant differences between normal conditions and CNQX in the VL or normal conditions and KA lesions in the VL, *t* test. B: electromyographic (EMG) activity of m. triceps brachii of cat A 37 days before lesions in the VL (black line shows normal condition data) and on days 2, 3, and 5 after the lesions (gray lines show postlesion data). The left panel shows data for locomotion on the flat surface, averaged over 17–29 strides for each day, and the right panel shows data for ladder locomotion averaged over 11–19 strides on each day. Error bars show SDs.

collected from 8 tracks in the lateral aspect of the anterior sigmoid gyrus in cat B (Fig. 1E). Neurons had a variety of somatosensory RFs: 10 responded to movement at the shoulder, 9 reacted to movement in the elbow joint, and 8

responded to movement of the wrist or pressure on the paw (Table 2).

Twenty-four neurons were identified as pyramidal tract projecting neurons (PTNs; Table 2), and three were identified as projecting to the red nucleus (cortico-rubral). Axonal conduction velocities of PTNs ranged between 10 and 74 m/s, and according to the criteria of Takahashi (103), 15 PTNs with axonal conduction velocities of 29–74 m/s were considered fast-conducting, whereas 9 PTNs with axonal conduction velocities of 10–21 m/s were considered slow-conducting (see also Ref. 50).

On each experimental day, responses of 1–3 neurons to inactivation of part of the VL with CNQX were tested. For five neurons recorded in cat B, the effects of two consecutive CNQX injections in different medial and lateral VL areas were tested. Altogether, the effect of inactivation of a part of the VL on the activity of motor cortex neurons was examined 40 times.

Neuronal activity under normal conditions.

An example activity of a typical neuron is shown in Fig. 3, A–E. This neuron (cell no. 5706) recorded in cat B was located laterally in the anterior sigmoid gyrus (Fig. 1E). In the resting cat, the neuron was activated by right elbow flexion. The activity of the neuron during standing was 1.7 ± 2.3 spikes/s. During locomotion on the flat surface, its activity was strongly modulated with the rhythm: it peaked at 15 spikes/s around the transition from swing to stance and was 2 spikes/s in the beginning of the swing (Fig. 3A, left side of the bottom trace). The raster in Fig. 3B shows that the activity of the neuron was consistent across many strides ($n = 70$). The activity is summed in Fig. 3C, which shows distribution of discharge frequency across the step cycle of flat surface locomotion. The period of elevated firing (PEF) is indicated by a black horizontal bar, and the preferred phase of the activity (PrPh) is depicted with a white circle and given in the right top corner of the panel along with the value of the dM. A rainbow bar below the graph shows the average discharge frequency in each 1/20th portion of the step cycle, color coded according to the scale at the bottom of the figure. During ladder locomotion, the discharge of the neuron throughout the step cycle was higher, particularly during the late swing phase, when it peaked at 35 spikes/s (Fig. 3, A, D, and E). The PrPh was the same as on the flat surface, whereas the dM was lower (see METHODS for statistical criteria).

The activity of this population of neurons during locomotion in normal conditions was described in our recent report (Appendix in Ref. 78); therefore, only activity characteristics that are directly relevant to the present study are given here. During locomotion on the flat surface, the average discharge rate of neurons was 13.7 ± 10.1 spikes/s, and the discharge of 89% (32/35) of cells was modulated with the rhythm. The dM was 9.0 ± 4.2 . The PEFs were $60 \pm 15\%$ of the step cycle long and were distributed over the cycle (Fig. 4A1). PEFs of different neurons overlapped, so that 55%–75% of neurons were simultaneously active in all phases of the cycle (Fig. 4A3). Because neurons were slightly more active during the swing than stance phase (Fig. 4A2), the population was slightly more active during swing than stance ($P = 0.007$, *U* test; Fig. 4A4).

Table 1. Characteristics of locomotion behavior

	Parameters of Strides	Temporary Inactivation in the VL		Permanent Lesions in the VL	
		Before	During	Before	After
Flat surface locomotion	Number of passages	30±7	31±5	26±7	27±4
	Number of strides	78±24	81±17	66±27	63±16
	Duration of stride, ms	706±72	722±59	600±51	581±58
	Duration of swing, ms	294±34	289±39	233±34	245±27
	Duration of stance, ms	412±51	433±32	367±39	336±38†
	Stride duty factor, %	58.4±3.2	60.1±2.9	61.3±4.3	57.8±2.7†
Ladder locomotion	Number of passages	31±6	32±4	27±6	29±4
	Number of strides	57±27	62±29	43±18	57±22
	Duration of stride, ms	666±87	658±99‡	548±76‡	547±77‡
	Duration of swing, ms	291±46	282±55	228±28	233±20‡
	Duration of stance, ms	375±58‡	377±62‡	320±58‡	313±74‡
	Stride duty factor, %	56.2±4.0‡	57.0±4.9‡	58.1±4.0‡	56.6±6.3

VL, ventrolateral thalamus. Bold type indicates statistical significance: Values that are statistically significantly greater during temporary inactivation or after permanent lesions in the VL than in normal conditions (Student's unpaired *t* test for averages, means ± SD); † values that are statistically significantly smaller after permanent lesions in the VL than in normal conditions; ‡ values that are statistically significantly smaller during locomotion on the ladder than on the flat surface.

Upon transition from the flat surface to accurate stepping on the ladder, 89% (31/35) of neurons changed activity, typically in two to three aspects. The mean discharge rate of 60% (21/35) and the dM of 54% (19/35) of cells changed (Fig. 5, A and B). The number of PEFs changed in 26% (9/35) of neurons, and the PEF duration changed in 23% (8/35). Changes in PrPh were least frequent (Fig. 5C). Despite the great majority of neurons showing significant activity differences between flat surface and ladder locomotion, the discharge rate of the entire population at 15.4 ± 8.6 spikes/s, the dM at 9.7 ± 4.2 , and the duration of PEF at $59\pm 20\%$ were similar between the tasks ($P > 0.05$, *U* test). This was because similar numbers of neurons changed activity in opposing directions. However, the recruitment of neurons at the end of stance (Fig. 4, A1, A3 and B1, B3) and the average discharge rate during stance (Fig. 4, A2, A4 and B2, B4) were slightly higher than on the flat surface, the latter by 3 spikes/s ($P < 0.001$, *U* test).

These population activity characteristics are consistent with previously reported data (34, 49–52, 80), suggesting

that the group of 35 neurons whose responses to temporary inactivation of part of the VL are described here are a representative group.

Reorganization of the activity of individual neurons in the motor cortex during temporary inactivation of a part of the VL.

A typical response of a motor cortical neuron (cell no. 5706) to inactivation of 10% of the VL (the estimated volume of the inactivation, see Verification of the effect of CNQX in the VL section above) with CNQX is shown in Fig. 3, F–J. This is the same cell the activity of which before inactivation is shown in Fig. 3, A–E. Immediately after 2 mL of 7.4 mM CNQX was injected into a lateral VL area (Fig. 1G), the activity of the neuron during standing decreased (to 0.3 ± 0.5 spikes/s; $P = 0.0001$, *t* test). The activity during locomotion was still sharply modulated with the rhythm and consistent across many strides (Fig. 3, F–J). However, the peak discharge on the flat surface was now only 8 spikes/s, half of that before the injection. On the ladder, the peak discharge decreased only slightly, but the activity diminished significantly during stance. The dM became greater during both tasks, whereas the PrPh did not change. Over the next 4 h, the activity of the neuron returned close to the baseline levels. The shape of the neuron's spike did not change over the period of observation (insets in Fig. 3, C–E, H–J, and M–O).

As described by Beloozerova and Marlinski (78), temporary inactivation of 10% of the VL led to a reduction of the discharge rate of half the neurons in layer V of the motor cortex during both flat surface and ladder locomotion. In individual neurons, the decreases ranged between 22% and 92%, and the activity of the population decreased by 4–5 spikes/s. However, in some neurons, inactivation in the VL led to an increase rather than decrease of activity. These increases, albeit seen less frequently than the decreases, could be substantial. An example is shown in Fig. 6. Here, before inactivation of a part of the VL, the neuron discharged throughout the step cycle during both flat surface and ladder locomotion, showing average discharge rates of 7.0 spikes/s and 16.4 spikes/s, respectively. The activity peaked at 18 spikes/s during flat surface locomotion and at 34 spikes/s during ladder

Table 2. Neurons analyzed

	Temporary Unilateral Inactivation in the VL with CNQX	KA Lesions in the VL Bilaterally	
		Before	After
Shoulder-related RF	10	22	26
Elbow-related RF	9	12	15
Wrist/paw-related RF	8	18	18
Two/three segment RF		3	1
No RF		10	
RF not tested	8	16	5
Total	35	81	65
Fast PTNs	15	47	34
Slow PTNs	9	25	21
PTN/Red nucleus		7	9
Cortico-rubral	3	1	3
noID axon	8		
Total	35	73	58

CNQX, 6-cyano-7-nitroquinoxaline-2,3-dione; KA, kainic acid; noID, neuron whose projections were not identified; PTN, pyramidal tract-projecting neuron; RF, receptive field; VL, ventrolateral thalamus.

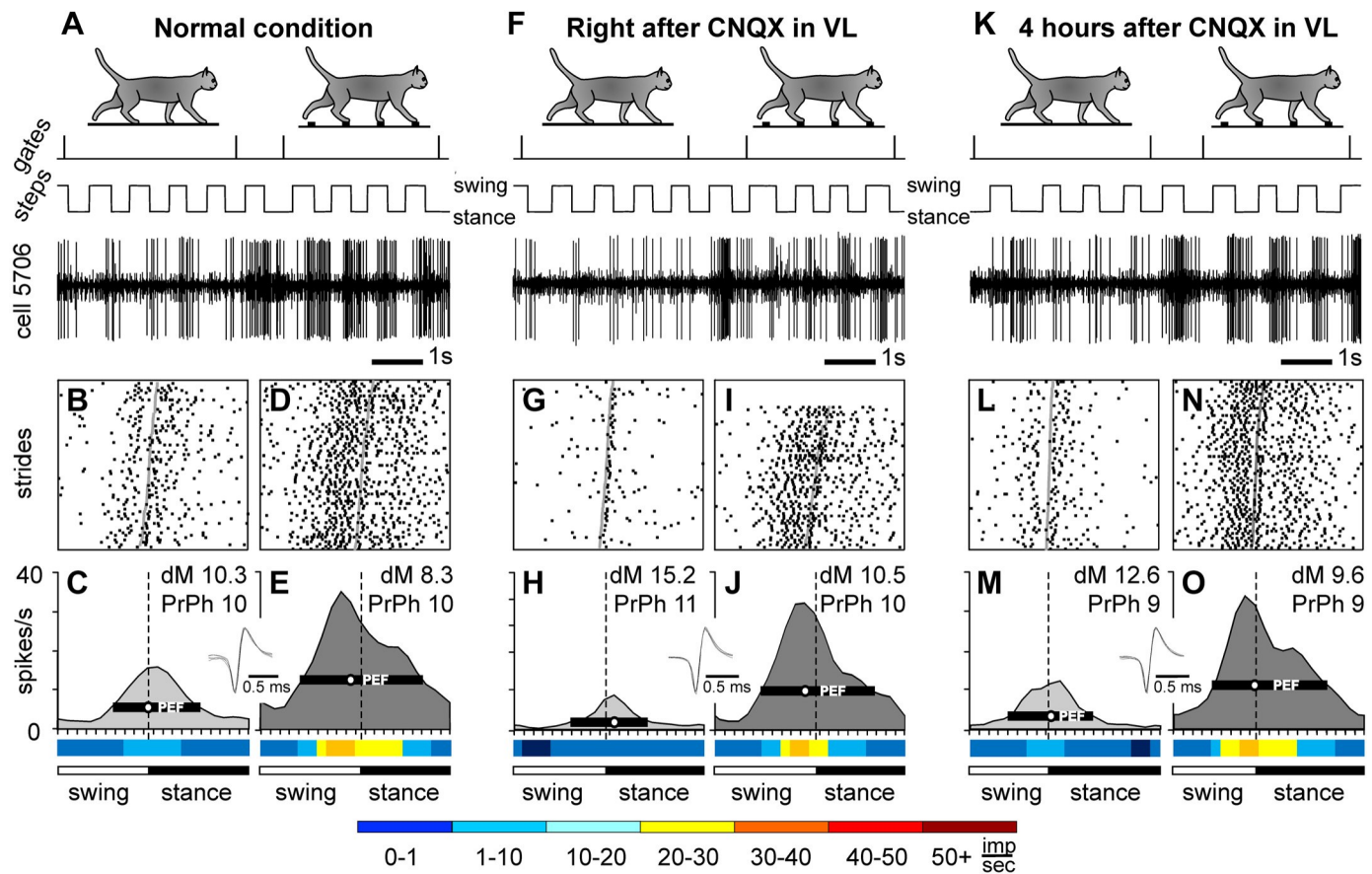
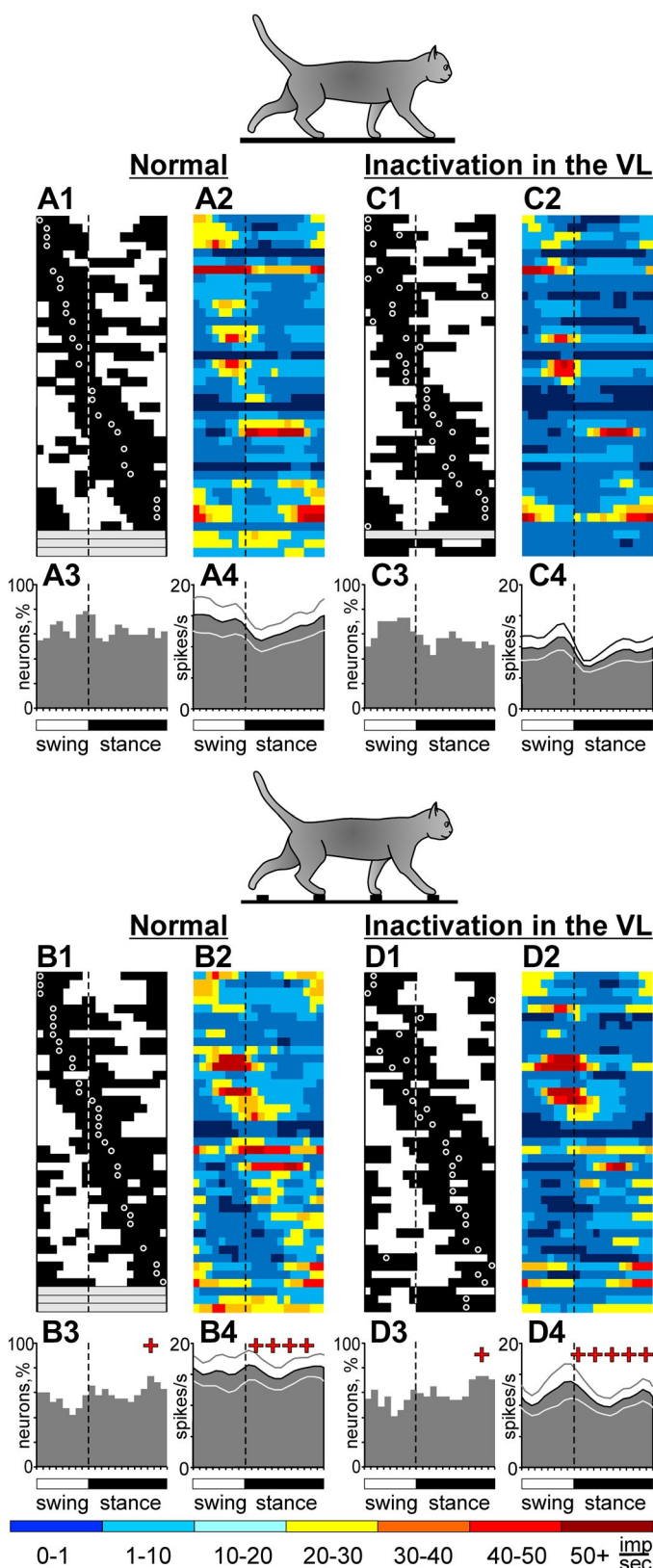


Figure 3. Effect of 6-cyano-7-nitroquinoxaline-2,3-dione (CNQX) application in the ventrolateral thalamus (VL) on the locomotion-related activity of an example motor cortical neuron (cell no. 5706). In the experiment, 2 mL of 7.4 mM CNQX was injected into the left VL of cat B (a lateral track), and the neuron was recorded in the lateral aspect of the left anterior sigmoid gyrus. Representative recordings of the activity of the neuron during flat surface and ladder locomotion before (A–E), immediately after (F–J), and 4 h after (K–O) the CNQX injection. For each group of panels, silhouettes of cats on the top indicate locomotion on the flat surface (left) and ladder (right). In A, F, and K, periods of flat surface and ladder locomotion are marked with vertical ticks on the trace “gates”; the trace “steps” indicates the swing and stance phases of the stride of the right forelimb; and the trace “cell 5706” shows a raw recording from the neuron. Rasters show the occurrence of spikes during 70 strides on the flat surface (B, G, and L) and ladder (D, I, and N). Area histograms show the average discharge rate of the neuron across the step cycle on the flat surface (light gray) and the ladder (dark gray) before (C and E), immediately after (H and J), and 4 h after (M and O) CNQX injection in the VL. Insets: five superimposed traces of individual spikes recorded during each condition. Rainbow bars below the histograms show the average discharge frequency of the neuron in each 1/20th portion of the step cycle, color-coded according to the scale at the bottom of the figure. dM, depth of modulation; PrPh, preferred phase.

locomotion (Fig. 6, A–E). After CNQX injection in the VL, the activity during both tasks changed, but in opposite directions (Fig. 6, F–J). During flat surface locomotion, the discharge rate decreased by 80% to 1.6 spikes/s and the peak firing decreased by 52% to 8.6 spikes/s (Fig. 6, G and H). In contrast, during ladder locomotion, the average and peak discharge rates increased by 34% to 22 spikes/s and by 62% to 55 spikes/s (Fig. 6, I and J). The dM increased during both tasks. Four hours after CNQX injection, the neuron activity returned close to the baseline (Fig. 6, K–O). The PrPh of the activity was not altered by VL inactivation during either task.

As seen in this and the previous example (Fig. 3) and described in detail by Beloozerova and Marlinski (78), changes in the discharge rate of individual neurons after inactivation of a part of the VL were almost always nonuniform across the step cycle. For example, the activity of the neuron shown in Fig. 6 during flat surface locomotion was affected the most during swing when it almost entirely disappeared, whereas in the beginning of stance, some activity

remained (Fig. 6, G and H vs. Fig. 6, B and C). We grouped all changes in the discharge rate into six groups (Supplemental Fig. S1; Supplemental Material is available at <https://doi.org/10.6084/m9.figshare.16441869>). Group 1 includes changes that peak during the stance-to-swing transition, group 2 includes those in which the change is maximal during swing. In group 3, the changes peak during swing-to-stance transition, in group 4, they are maximal during stance. Group 5 includes cases in which the increase in activity dominates, it often peaks during the swing-to-stance transition phase. Finally, group 6 includes changes that peak twice per step cycle. In the study by Beloozerova and Marlinski (78), these changes were interpreted as evidence of the VL contribution to the activity of motor cortical neurons. Here, we consider them directly as changes in the discharge rate that occur in response to inactivation in the VL. For 88% (35/40) of the cases examined during flat surface locomotion and for almost every case (95%, 38/40) tested during ladder locomotion, the change of the discharge rate was nonuniform



across the step cycle (78). This nonuniformity resulted in the activity of some neurons increasing at the phases of the cycle when it decreased in other neurons, potentially compensating for each other's effects at the population level. The nonuniformity in the activity change led to changes in the dM. The dM increased in half of neurons during flat surface locomotion and one-third of cells during ladder locomotion (not statistically different proportions). In addition, the pattern of the activity of a number of neurons changed. We will argue in the DISCUSSION that the opposing changes in the discharge rate of individual neurons and the increase in the dM have likely contributed to the maintenance of successful ladder locomotion when part of the VL was inactivated.

Individual neurons retain their ability to respond to the demand for movement accuracy on the ladder during inactivation of part of the VL but change the manner of the response.

When 10% of the VL was inactivated, in 93% (37/40) of cases, neurons still responded to the accuracy demand of the ladder task by changing activity upon transition from the flat surface to the ladder. Like in normal conditions, the activity typically altered in several respects. In 63% (25/40) of cases, the mean discharge rate changed, increasing in 18 and decreasing in 7 cases ($P < 0.05$, t test; Fig. 5D). The dM changed in 60% (24/40) of cases, increasing in 13 and decreasing in 11 (Fig. 5E). The number of PEFs changed in 33% (13/40) of cases,² and the duration of the PEF changed in 28% (11/40) of cases. The above proportions were similar to those seen in normal conditions. The differences were as follows. Unlike in normal conditions, when PEFs tended to become shorter during locomotion on the ladder compared with the flat surface, when part of the VL was inactivated, neurons had longer PEFs as often as they did shorter ones on the ladder. In addition, whereas in normal conditions only a few cells with a single PEF changed the preferred phases of activity (Fig. 5C), now half (14/26) of such cells did, although the change was usually small (1/10th of the step cycle; Fig. 5F).

Fn2

Figure 4. Motor cortex population activity characteristics during flat surface and ladder locomotion in normal conditions and during temporary inactivation of approximately one-tenth of the ventrolateral thalamus (VL) with 6-cyano-7-nitroquinoxaline-2,3-dione (CNQX). Phase distribution of periods of elevated firing (PEFs) of neurons during flat surface (A1 and C1) and ladder (B1 and D1) locomotion. Each row represents the PEF of one cell. A circular mark on a PEF denotes the preferred phase for cells with a single PEF per stride cycle. Neurons are rank ordered so that those with PEFs earlier in the cycle are plotted at the top of the graph. Vertical interrupted lines separate the swing and stance phases. A2, B2, C2, and D2: corresponding phase distributions of discharge frequencies. The average discharge frequency in each 1/20th portion of the cycle is color-coded according to the scale shown at the bottom of the figure. Proportion of active neurons (neurons in their PEF) in different phases of the step cycle during flat surface (A3 and C3) and ladder (B3 and D3) locomotion. The mean discharge rates of neurons during flat surface (A4 and C4) and ladder (B4 and D4) locomotion. Thin lines show means \pm SE. Red crosses indicate periods of the stride when the activity during ladder locomotion was significantly higher ($P < 0.05$, U test) than during flat surface locomotion, 35 neurons, 40 tests.

²The number of PEFs changed in the following ways: In four neurons, two PEFs per stride on the flat surface were replaced with only one PEF per stride on the ladder, whereas in nine neurons, the opposite change occurred.

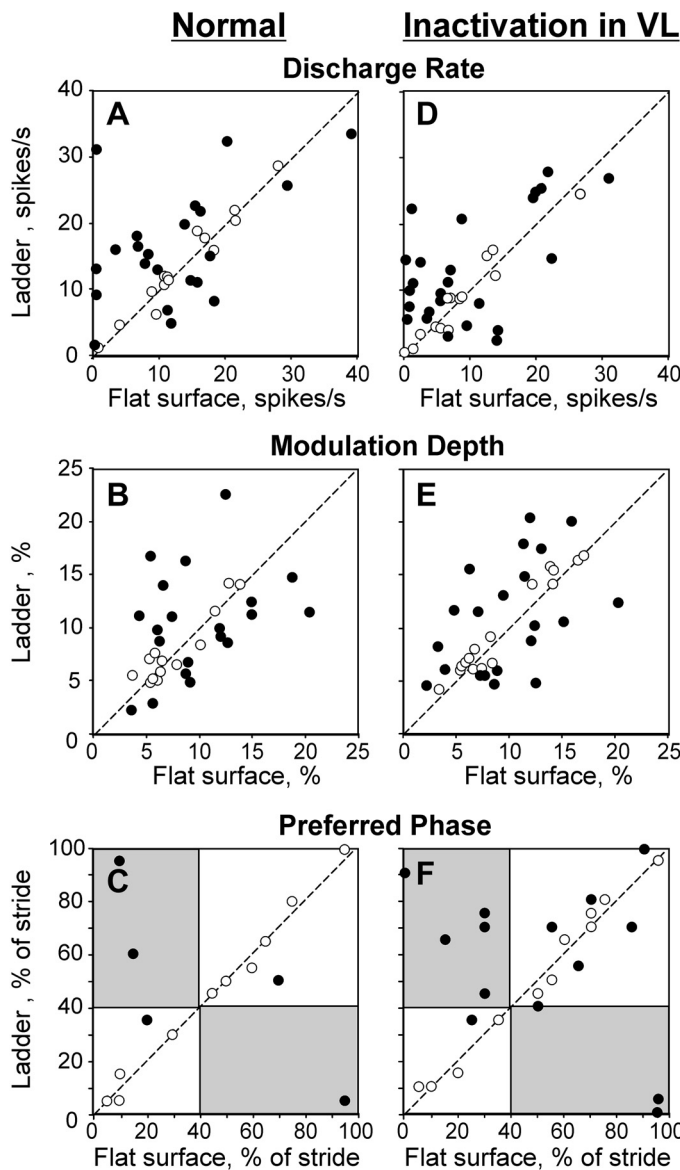


Figure 5. Responses of individual neurons to the ladder task in normal conditions (left three) and during temporary unilateral inactivation of a part of the ventrolateral thalamus (VL) with 6-cyano-7-nitroquinoxaline-2,3-dione (CNQX) (right three). The abscissa and ordinate of each point show the values observed during flat surface and ladder locomotion, respectively. Neurons with characteristics statistically significantly different between the two locomotion tasks (see METHODS) are shown with filled circles; the other ones are shown with open circles. A and D: mean discharge frequency averaged over the stride. B and E: depth of frequency modulation, dM. C and F: preferred phase of activity for neurons with a single period of elevated firing (PEF) during both locomotion tasks. Areas that correspond to the swing phase during one task but the stance phase during the other task are shaded.

Figure 7 schematically illustrates the typical effects of inactivation in the VL on the ability of neurons in the motor cortex to respond to the demand for stepping accuracy on the ladder. The first five examples show cases in which, after inactivation, neurons ceased responding to the ladder task by a change in the dM while still responding by an increase in the average discharge rate (panels 1–4) and typically also by changing some other activity characteristic (10 cases

total). Panels 6–10 show cases in which neurons only started responding to the ladder task by an increase in the dM when 10% of the VL was inactivated. In addition, they typically responded by a change in some other activity characteristics, not necessarily the same ones that they changed in normal conditions (12 cases total). The last four panels illustrate a variety of other dissimilar responses.

Except for four cases, including two cells that did not respond to the ladder task in either condition, all neurons responded, but they did so differently when 10% of the VL was inactivated compared with normal conditions. The dM response changed in 58% of cases (23/40). In 40% of cases, the way in which the pattern of the discharge (17/40) or duration of PEF (15/40) was modified changed. In 30% of cases, the discharge rate (13/40) or PrPh (12/40) was modified differently. We did not find any relationship between the responses of individual neurons to the ladder task under normal conditions and those when a part of the VL was inactivated.

The locomotion-related activity of the motor cortex layer V population is largely preserved during temporary inactivation of part of the VL.

Although most cortical neurons changed their activity during both flat surface and ladder locomotion after inactivation of 10% of the VL, many characteristics of population activity were preserved. On the flat surface, roughly as many neurons were active in most phases of the stride as in normal conditions (50%–70%; Fig. 4, C1 and C3). Moreover, relatively more neurons were active during the swing phase of the stride ($P < 0.0001$, Z test), a distribution more often seen for layer V neurons of the cat motor cortex compared with the nearly even distribution observed for this neuronal sample in normal conditions (e.g., see Refs. 34, 41, 51, and 52). Although the average discharge rate was 35% lower than normal (8.9 ± 7.8 spikes/s vs. 13.7 ± 10.1 spikes/s; $P < 0.0001$, t test), the population activity was still modulated with the rhythm as normal, showing an increase during swing and decrease in the beginning of stance (Fig. 4, A2, A4 and C2, C4).

The responses of the population to the demand for accuracy on the ladder were also preserved. Namely, upon transition from the flat surface to the ladder, as in normal conditions, the number of neurons active at the end of stance increased, and the discharge rate of the population increased during stance by a similar amount of 3 spikes/s ($P < 0.001$, U test; Fig. 4, C2, C4 and D2, D4).

Reorganization of the activity of motor cortex populations related to the shoulder, elbow, and wrist/paw.

Subpopulations of neurons with RFs on different segments of the right forelimb, i.e., subpopulations that are believed to control the movement of different limb segments, maintained their locomotion-related activity to a different degree when a part of the VL was inactivated. On the flat surface, the discharge rate of the wrist/paw-related group was fully preserved, remaining at 10 spikes/s. The elbow-related group tended to lose activity, going from 16.4 ± 16.7 spikes/s to 9.7 ± 11.4 spikes/s. In contrast, the discharge rate of the shoulder-related group decreased by 45% (from 13.0 ± 3.9 spikes/s to 6.9 ± 3.5 spikes/s; $P = 0.002$, U test). However,

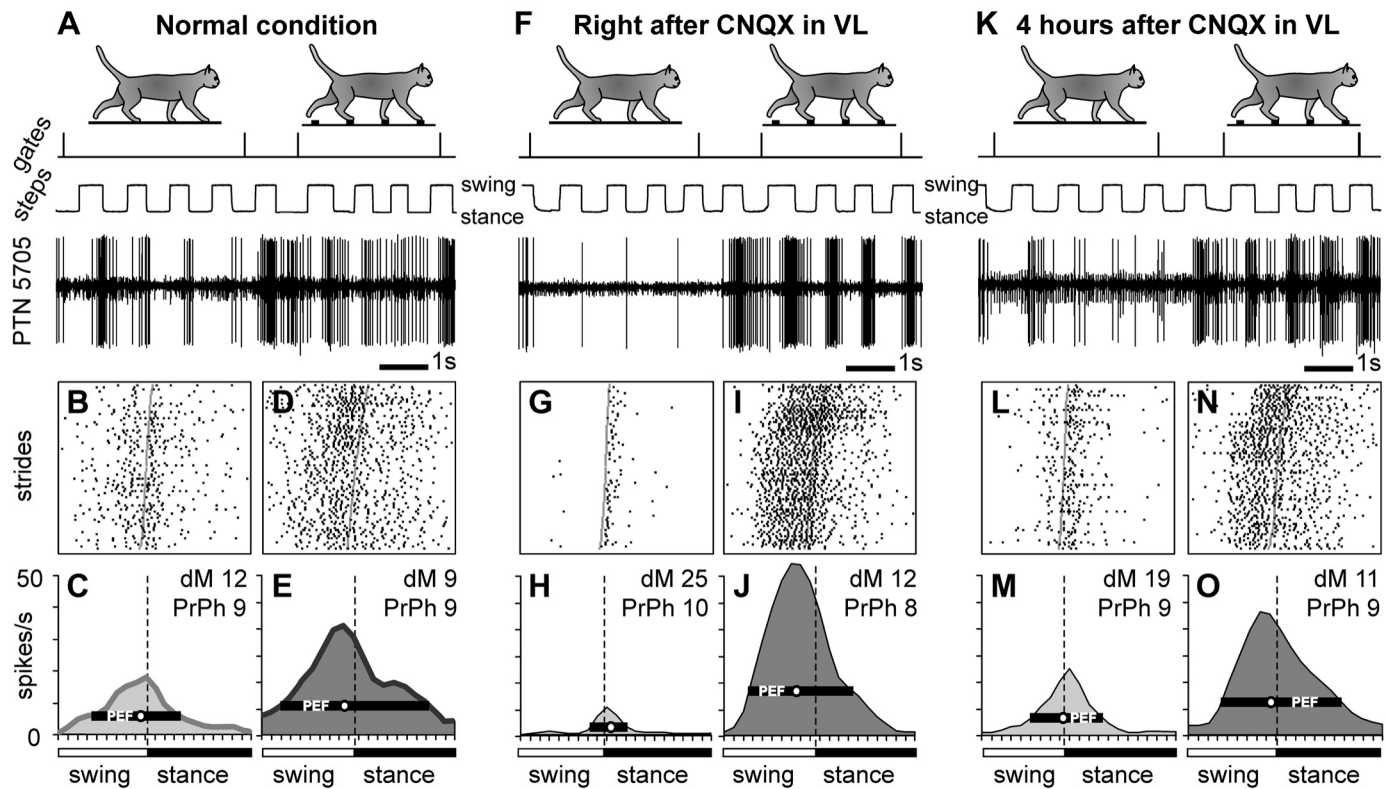


Figure 6. Example of a neuron, the activity of which increased during locomotion on the ladder after inactivation of a part of the ventrolateral thalamus (VL) with 6-cyano-7-nitroquinoxaline-2,3-dione (CNQX). Activity of a fast-conducting pyramidal tract projecting neuron (PTN) with a somatosensory receptive field (RF) on the elbow is shown. After 2 mL of 7.4 nM CNQX was injected into the ipsilateral VL (a medial track), the discharge rate of the neuron decreased during locomotion on the flat surface but increased during locomotion on the ladder. The activity of the neuron during flat surface and ladder locomotion is shown before (A–E), right after (F–J), and 4 h after (K–O) the injection. Rasters show the occurrence of spikes during 80 strides on the flat surface (B, G, and L) and ladder (D, I, and N). The average discharge rate of the neuron throughout the step cycle on the flat surface (light gray area histogram) and the ladder (dark gray area histogram) before (C and E), 40 min after (H and J), and 4 h after (M and O) CNQX injection in the VL. Other designations are as in Fig. 3. dM, depth of modulation; PrPh, preferred phase.

group activity profiles were preserved in all subpopulations (Fig. 8, A1, A2–C1, C2).

The normal or close-to-normal average discharge rates and normal profiles of group activity during locomotion on the flat surface must have helped the elbow- and wrist/paw-related subpopulations to respond nearly normally to the demands of the ladder task and support successful locomotion on the

ladder when a part of the VL was inactivated. Upon transition from the flat surface to the ladder, the activity of the wrist/paw-related group increased throughout the step cycle while still peaking at the end of swing (Fig. 8, C2 and C4). This was similar to their response in normal conditions (Fig. 8, C1 and C3). The average discharge rate of the wrist/paw population on the ladder was also normal. The activity of the elbow-

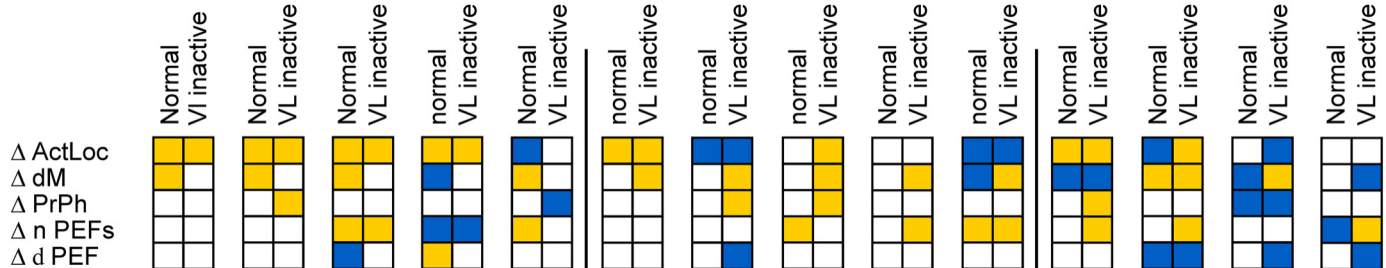
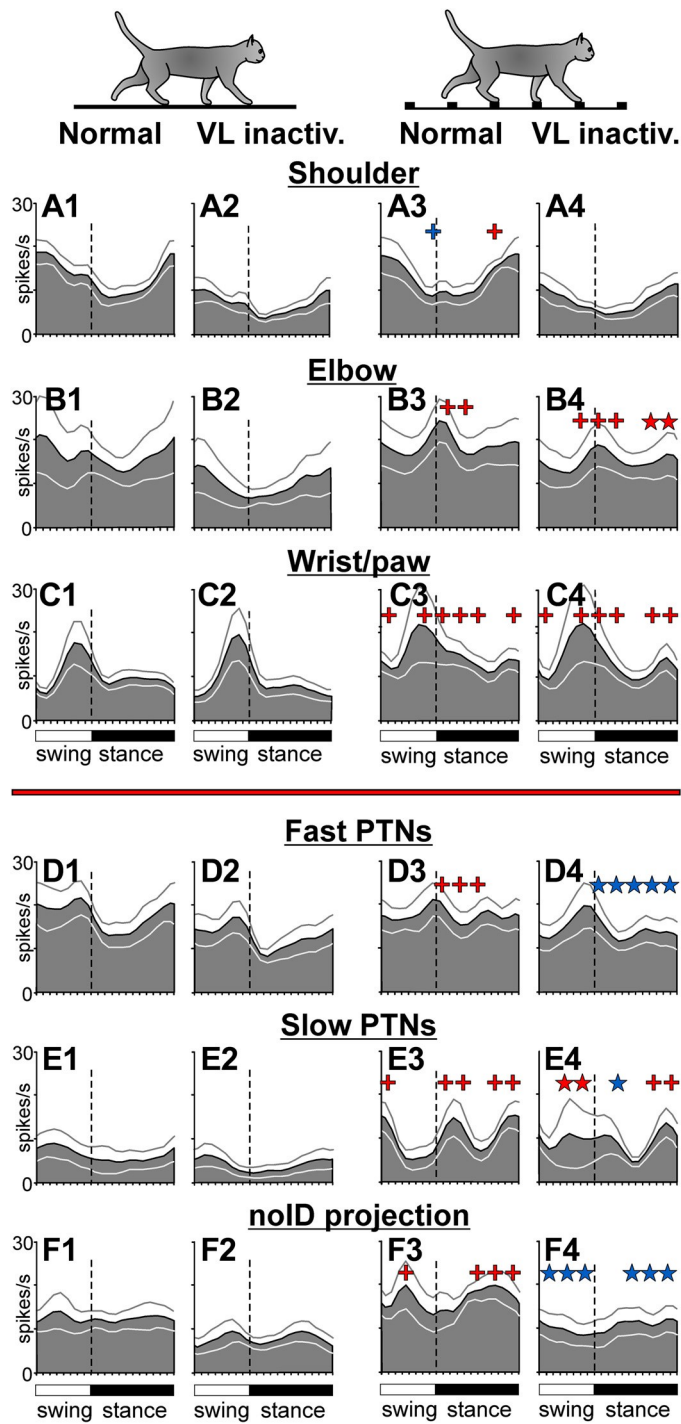


Figure 7. Graphical summaries of 14 pairs of representative responses of motor cortical neurons to the ladder task in normal conditions and during inactivation of part of the ventrolateral thalamus (VL) with 6-cyano-7-nitroquinoxaline-2,3-dione (CNQX). In each panel, changes in the activity of a neuron upon transition from flat surface to ladder locomotion in normal conditions and during inactivation in the VL are shown by two adjacent columns of five squares each. The left column graphically summarizes changes in the activity characteristics in normal conditions; from top to bottom: average discharge rate (DActLoc), depth of modulation (dM), preferred phase (PrPh), number of period of elevated firings (n PEFs), and duration of PEFs (d PEF). The right column summarizes changes in these activity characteristics upon the transition during inactivation of a part of the VL. Yellow designates a statistically significant increase in the value of the parameter, blue designates a decrease in the value, and open squares denote no change. See the text for further details.

related group changed by forming a prominent peak during the swing-to-stance transition (Fig. 8, B2 and B4), which was similar to their response in normal conditions (Fig. 8, B1 and B3). In addition, this group increased its activity at the end of stance by 4 spikes/s ($P = 0.012$, U test), a response not seen in normal conditions. The average discharge rate of the elbow-related population was normal. Unlike these two groups, which showed normal or close to normal responses to the ladder task when a part of the VL was inactivated, the shoulder-related group did not respond (Fig. 8, A2 and A4).



This was different from how this group behaved in normal conditions (Fig. 8, A1 and A3). Thus, the success of the accurate stepping on the ladder when part of the VL was inactivated appeared to rely on the essentially normal activity of the wrist/paw- and elbow-related motor cortex subpopulations, whereas the shoulder-related group did not contribute.

Reorganization of the activity of motor cortex efferent populations during temporary inactivation of a part of the VL.

Different efferent subpopulations of the motor cortex also differed in their ability to maintain locomotion-related activity when 10% of the VL was inactivated. On the flat surface in normal conditions, the activity of fast-conducting PTNs was 18 spikes/s, and was step-cycle modulated with a peak in the swing phase (Fig. 8D1). Upon transition to the ladder, the average discharge rate of this group did not change, but the activity became more evenly distributed over the step cycle because of an increase in the first half of stance (Fig. 8D3). When part of the VL was inactivated, the average discharge rate was preserved during both tasks, and was still similar between them (Fig. 8, D1–D4). However, the activity did not evenly distribute across the step cycle during ladder locomotion; instead, it remained modulated, showing a peak in late swing (Fig. 8, D2 and D4).

At variance, the activity of slow-conducting PTNs during locomotion on the flat surface in normal conditions was 7 spikes/s, less than half of that of fast-conducting PTNs, and was not modulated as much (Fig. 8E1). Upon transition to the ladder, however, it increased, particularly during swing-to-stance and stance-to-swing transitions, and became sharply modulated (Fig. 8E3). Inactivation of 10% of the VL did not prevent this group from increasing their overall discharge throughout the step cycle upon transition to the ladder. However, it led to a reduction of the activity peak in

Figure 8. Phase distributions of average discharge frequencies of groups of neurons with somatosensory receptive fields (RFs) on different segments of the forelimb, as well as those of pyramidal tract projecting neurons (PTNs) with different axonal conduction velocities and of a group of neurons for which the destination of the axon was not identified. Data for flat surface locomotion (left two columns) and ladder locomotion (right two columns) in normal conditions and during inactivation of approximately one-tenth of the ventrolateral thalamus (VL) with 6-cyano-7-nitroquinoxaline-2,3-dione (CNQX) are shown. A: activity of neurons responsive to passive movement in the shoulder joint in normal conditions (A1 and A3) and after inactivation in the VL (A2 and A4; $n = 10$). B: activity of neurons responsive to passive movement in the elbow joint or palpation of arm muscles ($n = 11$, 2 cells whose responses to inactivation of two different VL areas were tested are included twice). C: activity of neurons responsive to passive movement in the wrist joint or palpation of muscles on the forearm or paw ($n = 11$, 3 cells whose responses to inactivation of two different VL sites were tested are included twice). D: activity of fast-conducting PTNs ($n = 19$, 4 neurons whose responses to inactivation of two different VL sites were tested are included twice). E: activity of slow-conducting PTNs ($n = 9$). F: activity of neurons with an unidentified axonal projection ($n = 9$, one neuron whose responses to inactivation of two different VL sites were tested is included twice). Red crosses indicate periods of the stride when the activity during ladder locomotion was significantly higher ($P < 0.05$, U test) than during flat surface locomotion. Blue cross indicates periods where it was smaller. Red stars show periods of the stride where the response of the population to the ladder task during inactivation of a part of the VL was significantly greater ($P < 0.05$, U test) than in normal conditions. Blue stars indicate those where it was smaller. Other designations are as in Fig. 4.

early stance, whereas the activity during midswing increased (Fig. 8E4). Thus, although the group activities of both fast- and slow-conducting PTNs were fairly resistant to inactivation in the VL, the average discharge rate was better preserved in each group than the group activity pattern. In both groups, the change in the activity pattern led to more firing during the swing than stance phase of the stride.

In contrast to PTNs, responses of the noID (neurons whose projections were not identified) group to the ladder task were severely affected by VL inactivation by being plainly abolished (Fig. 8, F2 and F4). Unlike in normal conditions (Fig. 8, F1 and F3), neither the activity peak during swing nor the peak during stance was present after inactivation in the

VL (Fig. 8, F2 and F4). In addition, the average discharge rate tended to be lower than normal by 37% ($P = 0.064$, t test).

Experiment with Bilateral Lesions in the VL with Kainic Acid

KA lesions in the thalamus.

Histological examination of the tissue harvested 42 days after KA injections in the VL revealed the following damage.

Left side. The medial part of the left VL between L3 and L5 was fully destroyed (Fig. 9B). Between L5 and L7, some of the ventrocaudal aspect of the VL survived (Fig. 9, C and D). In addition, at least some of the most lateral 0.5 mm of the

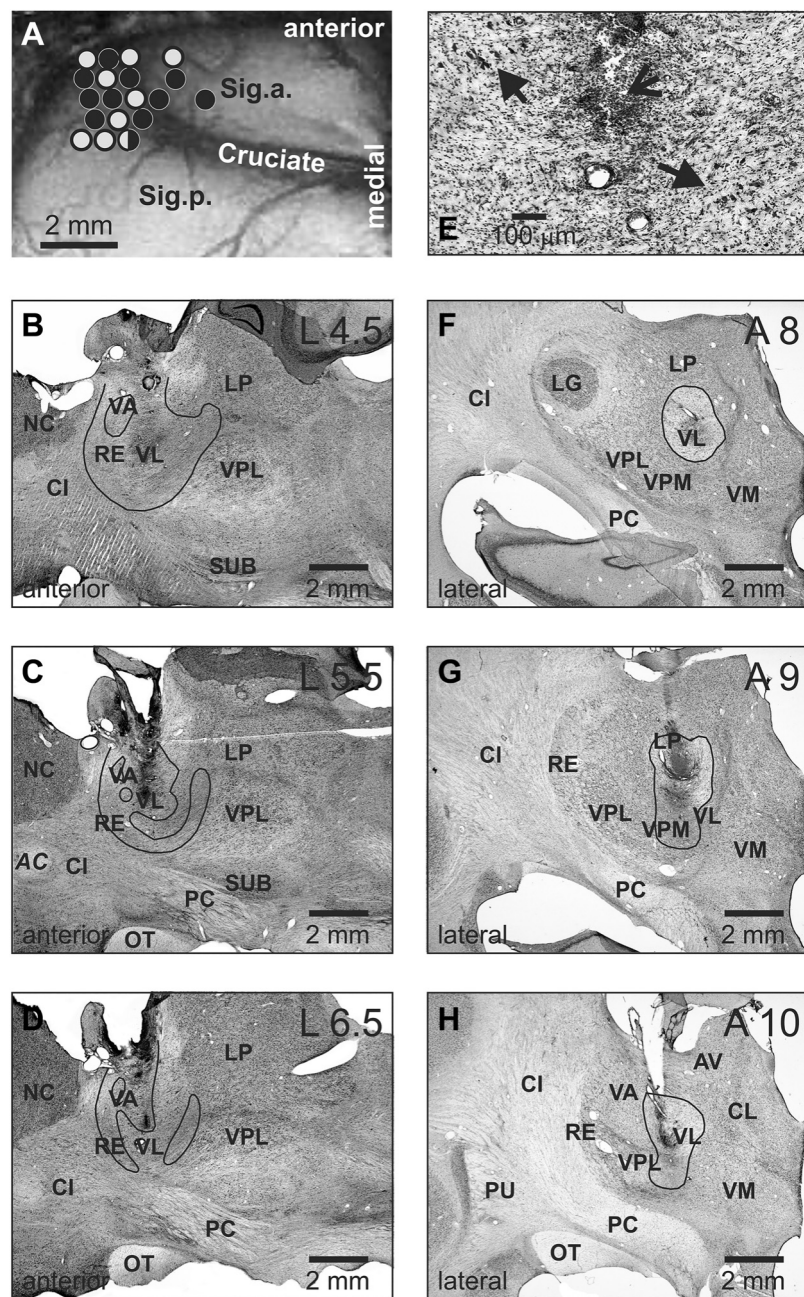


Figure 9. Reconstructions of recording sites in the motor cortex and lesion sites in the ventrolateral thalamus (VL) of cat A. A: sites of recording in the forelimb representation of the left motor cortex. Microelectrode entry points into the cortex that were made before the lesions are shown by black circles, while those made after the lesions are shown by open circles. B–D: parasagittal sections of the left thalamus. Areas where most cells were destroyed by kainic acid (KA) are outlined. The circled areas in the VA appeared intact. E: high magnification photomicrograph of a section through the lesion site in the left thalamus. An arrow with an open head points to the KA injection site. Arrows with solid heads point to several surviving neurons next to the KA injection site. F–H: frontal sections of the right thalamus. Areas where most cells were destroyed by kainic acid are outlined. B–H: cresyl violet stain. AC, anterior commissure; AV, nucleus antero-ventralis thalami; CI, capsula interna; CL, nucleus centralis lateralis; Cruciate, sulcus cruciatus; LG, lateral geniculate nucleus; LP, nucleus lateralis posterior; NC, nucleus caudatus; OT, optic tract; PC, pedunculus cerebri; PU, putamen; RE, nucleus reticularis thalami; Sig.a, gyrus sigmoideus anterior; Sig.l, gyrus sigmoideus lateral; Sig.p., gyrus sigmoideus posterior; SUB, nucleus subthalamicus; VA, nucleus ventralis anterior; VL, nucleus ventralis lateralis; VM, nucleus medialis; VPL, nucleus ventralis posterolateralis; VPM, nucleus ventralis posteromedialis.

VL probably survived. Overall, 75% of the left VL was lesioned. In addition, the RE between L4 and L7 was destroyed, and the VA between L4 and L6.5 was significantly damaged (Fig. 9, B–D). Other neighboring nuclei were much less damaged or were intact. A more detailed description of the lesion is provided in APPENDIX B.

Right side. The most caudal part of the right VL at A8.0–8.5 was nearly entirely damaged (Fig. 9F). More rostrally, at A9.0–10.0, only the lateral half of VL was lesioned, and significant parts of the nucleus ventralis posteromedialis (VPM) and nucleus ventralis posterolateralis (VPL) were damaged as well, along with the nucleus lateralis posterior (LP), which was damaged by the injection cannula (Fig. 9, G and H). The rostral one-third of the VL was largely intact, with no lesion observed rostrally to A10.5. We estimate that 50% of the right VL was lesioned. More details about the lesion are given in APPENDIX B.

Surviving neurons in the VL and their activity. Examination of the sections showed that the lesions were not uniform but contained islands of less affected tissue, particularly on the left side (Fig. 9, B–D). In addition, within the areas largely depleted of cell bodies, even right next to an injection site, there were many neurons with somatas that appeared normal (Fig. 9E). Microelectrode recordings from both the left and right VL conducted 1, 2, and 4 wk after KA injections showed that although there were far fewer active cells than before the injections, there were still some spontaneously active neurons, including neurons that responded antidromically to electrical stimulation of the motor cortex. The activity of a number of neurons tested during locomotion, including cortically projecting cells, was modulated with the locomotor rhythm.

Behavioral effects of KA lesions in the thalamus.

When isoflurane was discontinued after the end of KA injections in the VL, the cat started moving almost immediately but appeared unconscious for more than 7 h; it was very rigid and restless. The next morning, the cat was fully conscious but very quiet and slow moving. Locomotion on the flat surface appeared normal. Locomotion on the ladder was tested later that day, 30 h after the injection. The cat had a normal appetite but still appeared weak. During the first few runs along the ladder, it missed most crosspieces and stepped between them. Within several minutes, however, ladder locomotion dramatically improved, and during the following passages, the cat only occasionally placed its right forepaw on the edge of a crosspiece, which is not normal for cats, and on several occasions completely missed the crosspieces. Normally, cats nearly always step on the flat top of the crosspiece and never miss a crosspiece.

On day 2 after the injections, the cat continued walking well on the flat surface while having difficulties on the ladder. On the ladder, it often placed paws, except the left forepaw, on the edge of a crosspiece, and occasionally missed a crosspiece with its right forelimb or left hindlimb. The right forelimb missed because its strides were occasionally too short. However, during a number of strides that were going to be too short, the cat corrected itself in midswing and stepped successfully on the crosspiece. It is unclear whether this underreaching was due to muscle weakness, miscalculation, or both. In addition, at the beginning of the day, the cat

often stepped on the same crosspiece with two paws of the same girdle simultaneously, which cats normally do very rarely, only when they hesitate. Ordinarily, cats step on each crosspiece with only one forepaw (Fig. 1A) and then one hindpaw. Throughout day 2, the cat appeared to use a special effort to step on the crosspieces, and ladder locomotion was slower than normal. The EMG activity of the elbow extensor *m. triceps brachii* (Fig. 2B) and the knee extensor *m. vastus lateralis* (not illustrated) was largely normal, only slightly elevated at the peak ($P < 0.05$, *t* test; light gray traces in Fig. 2B).

On the third day, the cat was no longer missing the ladder's crosspieces. It placed paws normally on the tops of the crosspieces, only occasionally stepping on an edge with a hindpaw. The EMG activities of both recorded muscles showed no statistical difference from normal (Fig. 2B). However, the cat still appeared to need extra effort to walk on the ladder. No abnormalities were seen on the fourth day or throughout the rest of the observation.

Behavioral examination of the effectiveness of KA lesions in the thalamus, the muscimol test.

To assess the effectiveness of KA lesions of the VL, injections of muscimol, a selective agonist for GABA receptors, were administered in the VL 3–17 days before and 30–32 days after the KA lesion. As explained in METHODS, we reasoned that an injection of muscimol in the intact VL would compromise locomotion on the ladder but not result in any deficits if the VL was already lesioned by KA, thereby confirming the lesion.

Left side. The effect of muscimol injection in the left VL before KA lesions was as follows. Fifteen minutes after the end of the injection, the cat walked normally on both the flat surface and the ladder. One hour later, however, the cat occasionally started placing its right forepaw on the farther edge of the crosspieces, and even missed a crosspiece a few times. This deficit continued over the next 2 h of observation, and was very mild: in 99 rounds of locomotion that consisted of 450 ladder steps, the cat only missed a crosspiece on 12 steps, typically at the beginning of the ladder. Flat surface locomotion was not affected. There was no activity in the VL 0.72 mm away from the injection site. The activity of several neurons recorded in the motor cortex was step-cycle modulated. The next morning, the cat walked normally both on the flat surface and the ladder.

The effect of a similar muscimol injection in the left VL 1 mo after the KA lesions was very similar, if not slightly more severe. Starting 15 min after the injection, and over the next 2 h, the cat often placed right paws on the farther edge of the crosspiece when walking on the ladder and occasionally missed a crosspiece. Locomotion on the flat surface was normal.

Right side. The effect of the injection of muscimol in the right VL before KA lesions was as follows. Thirty minutes after the end of the injection, when walking on the ladder, the cat missed a crosspiece by its left hindpaw a few times because of taking too large a step. The ladder locomotion worsened over the next 2 h, when the cat started missing nearly every crosspiece with its left hindpaw because of taking too large steps. At that time, the cat also missed a crosspiece a few times with its left forepaw. Locomotion on the

flat surface was not affected. There was no activity in the VL 1.0 mm caudally to the site of the injection. The activity of several neurons recorded in the motor cortex was step-cycle modulated. The next morning, the cat walked normally, both on the flat surface and the ladder.³

The effect of a similar muscimol injection in the right VL 1 mo after the KA lesions was similar. When walking on the ladder immediately after the injection, the cat always placed its left hindpaw and often left forepaw on the farther edge of the crosspiece. However, only a few complete misses were observed, all by the left hindpaw. This test was conducted 2 days after the post-KA muscimol test in the left VL described earlier.

Thus, the results of the muscimol tests showed that despite substantial damage (Fig. 9, B–H), the VL was still contributing to the control of accurate stepping on the ladder after KA lesions about a month earlier.

Neurons analyzed before VL lesions.

Recordings of the firing activity during flat surface and ladder locomotion before KA lesions in the VL were obtained from 81 neurons. The neurons were recorded in the anterior aspect of the lateral sigmoid gyrus and in the lateral aspect of the anterior sigmoid gyrus (Fig. 9A). Twelve microelectrode tracks were used over a 3-mo period, yielding between 3 and 15 neurons each (6.7 ± 4.1 neurons per track).

The neurons had diverse somatosensory RFs (Table 2). Twenty-two had an RF that involved the shoulder: 20 responded to movement in the shoulder joint, and 2 had tactile RFs on the shoulder. Twelve neurons had an elbow-related RF: 9 reacted to movement in the elbow joint, and 3 had a tactile or deep RF on the arm. Eighteen cells had a wrist or paw-related RF: 13 responded to movement of the wrist, and 5 had a tactile or deep RF on the paw. RFs of 3 neurons spanned more than one segment of the right forelimb, and 10 neurons did not have a somatosensory RF that we could identify in the resting animal.

Seventy-two neurons were identified as PTNs, and one cell was identified as projecting to the red nucleus, a corticorubral neuron (Table 2). Axonal conduction velocities of the PTNs were in the range of 10–70 m/s, and 47 PTNs with a conduction velocity of 34–70 m/s were considered fast-conducting, whereas 25 PTNs with conduction velocities of 10–24 m/s were considered slow-conducting (50, 103). Axons of seven PTNs (six fast-conducting and one slow-conducting) gave off a collateral to the red nucleus.⁴ Conduction velocities of axons reaching the red nucleus were in the range of 12–60 m/s.

Neurons analyzed after VL lesions.

Recordings started on day 2 after the lesion, but only data obtained on day 8 and later are included in this report. Recall that starting on day 4, the cat locomotion appeared normal to a human observer. Thus, the data presented here reflect the activity of the motor cortex when compensation for the lesion in the VL was already sufficient to support

normal-looking behavior. Recording proceeded for 27 days and was obtained on 19 of the days. On average, 3.4 ± 1.6 (range 1–7) neurons were recorded on each day as the cat walked on the flat surface and the ladder. The activity of a total of 65 neurons was recorded using one of the same tracks and 8 immediately adjacent tracks, from which the activity of 81 neurons was recorded before the KA lesions (Fig. 9A). On average, 7.2 ± 4.1 neurons per track were recorded.

As before the lesions, the neurons had diverse somatosensory RFs (Table 2). Twenty-six responded to movement of the shoulder, 15 reacted to movement in the elbow joint, and 18 had a wrist- or paw-related RF: 17 responded to movement of the wrist and 1 had a tactile RF on the paw. RF of one neuron spanned more than one segment of the right forelimb.

Fifty-five neurons were identified as PTNs and three as projecting to the red nucleus (cortico-rubral neurons). Axonal conduction velocities of the PTNs were in the range of 8–75 m/s, and 34 PTNs with a conduction velocity of 28–75 m/s were considered to be fast-conducting, whereas 21 PTNs with conduction velocities of 8–24 m/s were considered slow-conducting (50, 103). Axons of nine PTNs (six fast-conducting and three slow-conducting) gave off collateral to the red nucleus. Axonal conduction velocities to the red nucleus were in the range of 8–75 m/s.

Overall, the composition of the neuronal group tested after the KA lesions in the VL was similar to that tested before the lesions.

Strides analyzed before and after VL lesions.

During recordings of the activity of each neuron included in the “before VL lesions” group, the cat walked around the chamber 10–45 times. From these rounds, 10–135 strides were selected for the analysis of the activity of each neuron during each locomotion task according to the criteria outlined in METHODS. Characteristics of the strides are shown in Fig. 2A and Table 1. The strides were 50 ms faster, and the stride duty factor was 5.3% smaller on the ladder than on the flat surface ($P < 0.001$, t test).

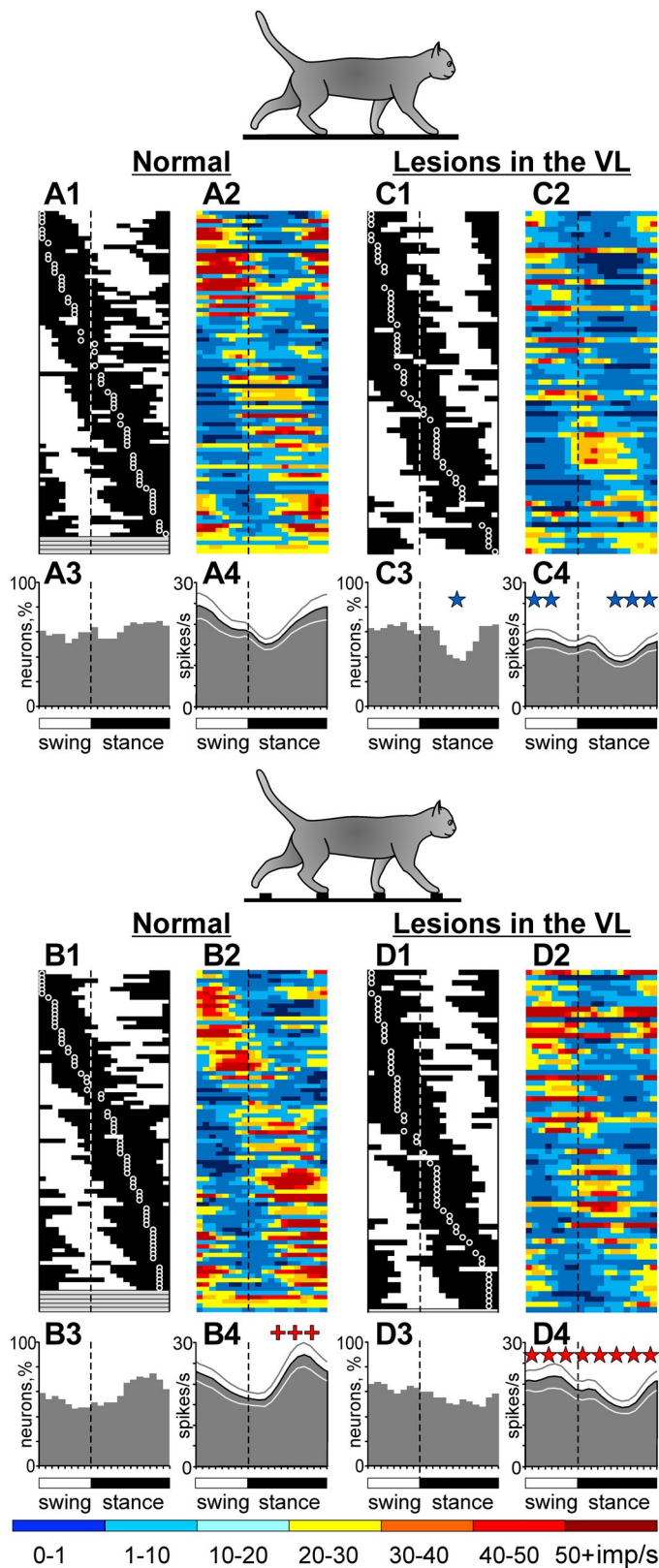
During recordings of the activity of each neuron included in the “after VL lesions” group, the cat walked around the chamber 15–35 times. From these trials, 23–111 strides were selected for the analysis of the activity of each neuron during each locomotion task. Both for flat surface and ladder locomotion, these strides were similar in duration to those recorded before VL lesions (Fig. 2A, Table 1). On the flat surface, however, the structure of the stride was slightly different, with the swing phase 5% longer and the stance phase 8% shorter ($P < 0.001$, t test). Consequently, the stride’s duty factor was 6% smaller than before the lesions. During ladder locomotion, the stride duty factor was similar to that before the lesions, and like in normal conditions, it tended to be slightly smaller than on the flat surface (Fig. 2A, Table 1).

Overall, the cat walked a similar number of times along each of the test corridors during the recording of the activity of neurons before and after the VL lesions. The strides

³A microelectrode left overnight in the VL in a cannula, adjacent to that through which muscimol was injected, recorded activity of multiple neurons the next morning. These neurons responded to somatosensory stimulation as they did the previous day before the injection, indicating VL recovery from muscimol.

⁴Latent periods of antidromic responses from the red nucleus were always longer (by 0.1–0.57 ms) than would be expected if the test stimulus exited the axon descending within the pyramidal tract rather than its collateral to the red nucleus.

on the flat surface were slightly different in the duration and temporal structure (duty factor), but they were similar on the ladder for the “before” and “after” VL lesion conditions.



Reorganization of the activity in the motor cortex after bilateral lesions of 50%–75% of the VL.

The activity of 81 neurons recorded before lesions in the VL was similar to that previously reported (34, 49–52, 80). Details of the locomotion-related activity of this neuronal population and the activity of subpopulations of these neurons grouped based on the destination of the axon, axon conduction velocity, and location of neuron’s somatosensory RF are given in APPENDIX A and illustrated in Fig. 10, A and B and Fig. 12, A1, A3–F1, F3. Because the great majority of neurons included in this sample were PTNs, to facilitate comparison of their activity with published data, we have compiled Table 3, which lists locomotion-related activity characteristics of fast- and slow-conducting PTNs in the before and after VL lesions groups in a format similar to that of published data from a larger neuronal sample obtained in normal conditions from several cats (Table 2 in Ref. 50). The main difference of cat A PTNs selected for the normal activity group in the present study was that they discharged at higher rates during both locomotion tasks compared with the rates of larger PTN populations previously collected and averaged across several cats.

After the VL was lesioned, the average discharge rate of neurons during locomotion on the flat surface declined by 28% to 14.4 spikes/s (compared with 20 spikes/s in normal conditions; $P = 0.007$, t test; Fig. 10, A2, A4 and C2, C4). The activity during the early swing and late stance suffered the most. This resulted in the population’s activity profile becoming less modulated, displaying a peak-to-peak range of only 5 spikes/s compared with 10 spikes/s in normal conditions. The pattern of neuronal recruitment also changed (Fig. 10, A3 and C3). Rather than being fairly evenly distributed over the step cycle, it became modulated with more neurons in their PEF during swing and fewer during mid-stance ($P < 0.022$, Z test). The activity of nearly every neuron was still modulated with the locomotor rhythm, showing the same number and duration of PEFs and the same dM (Table 3). We will argue below in DISCUSSION that this allowed the cortical network to effectively respond to the demand for accuracy in stepping when the cat transitioned to the ladder.

The motor cortex population responded differently to the ladder task after lesions in the VL than in normal conditions.

Figure 10. Population activity characteristics of neurons during flat surface and ladder locomotion before and after kainic acid (KA) lesions in the ventrolateral thalamus (VL). Phase distribution of periods of elevated firing (PEFs) of neurons during flat surface (A1 and C1) and ladder (B1 and D1) locomotion. A2, B2, C2, and D2: corresponding phase distributions of discharge frequencies. The average discharge frequency in each 1/20th portion of the cycle is color coded according to the scale shown at the bottom of the figure. Proportion of active neurons (neurons in their PEF) in different phases of the step cycle during flat surface (A3 and C3) and ladder (B3 and D3) locomotion. The mean discharge rate of neurons during flat surface (A4 and C4) and ladder (B4 and D4) locomotion. Thin lines show mean \pm SE. Red crosses indicate periods of the stride when the activity during ladder locomotion was significantly higher ($P < 0.05$, U test) than during flat surface locomotion. Red stars indicate periods of the stride when the response of the population to the ladder task after lesions in the VL was significantly greater ($P < 0.05$, U test) than in normal conditions, whereas blue stars indicate when it was weaker. Other designations are as in Fig. 4.

Table 3. Selected parameters of locomotion-related activity of fast- and slow-conducting PTN populations before and after KA lesions in the VL

Parameters of PTN Activity		Fast Conducting before VL Lesions	Fast Conducting after VL Lesions	Slow Conducting before VL Lesions	Slow Conducting after VL Lesions
		n = 47	n = 34	n = 25	n = 21
Standing	Proportion of cells with RFs, %	87.5	94	80	95
	Proportion of active cells, %	94	94	96	90.5
	Average activity, spikes/s	13.5 ± 1.2	10.9 ± 1.4	10.1 ± 1.2	6.8 ± 1.2
	Discharge variability, CV	3.7 ± 0.8	3.2 ± 0.6	1.0 ± 0.2	2.1 ± 0.8
Flat surface locomotion	Average activity, spikes/s	23.5 ± 2.1	16.6 ± 2.1	14.0 ± 1.8	11.9 ± 1.5
	Discharge variability, CV	2.5 ± 0.3	2.7 ± 0.3	2.3 ± 0.3	1.7 ± 0.2
	Proportion of modulated, %	96	100	92	100
	Proportion with zero spikes/s in any bin, %	6.4	5.9	8	19
	Mean peak rate, spike/s	54.3 ± 4.9	35.6 ± 3.7	27.4 ± 3.3	29.0 ± 2.5
	Depth of modulation, dM, %	10.2 ± 0.6	9.2 ± 0.6	9.3 ± 1.0	11.8 ± 1.2
	Coefficient of modulation, M, %	92.8 ± 1.4	90.4 ± 1.5	87.8 ± 3.1	92.9 ± 2.3
	Duration of PEF, % of cycle	60 ± 2.0	61.5 ± 2.0	62 ± 3.5	53 ± 3.5
	Proportion with one PEF, %	84	73	74	95
Ladder locomotion	Average activity, spikes/s	23.4 ± 2.0	22.5 ± 2.7	14.0 ± 1.8	13.1 ± 1.7
	Discharge variability, CV	2.3 ± 0.2	3.4 ± 0.4	2.2 ± 0.3	2.1 ± 0.2
	Proportion of modulated, %	100	100	96	95
	Proportion with zero spikes/s in any bin, %	8.5	3.0	8	19
	Mean peak rate, spike/s	58.3 ± 4.1	47.5 ± 5.1	36.4 ± 3.5	30.6 ± 3.1
	Depth of modulation, dM, %	11.8 ± 0.6	9.5 ± 0.6	9.6 ± 0.8	10.6 ± 0.9
	Coefficient of modulation, M, %	96.4 ± 1.0	91.6 ± 1.7	92.0 ± 1.9	93.7 ± 2.0
	Duration of PEF, % of cycle	58 ± 2.5	60.5 ± 2.5	58.5 ± 3.0	59.0 ± 3.5
	Proportion with one PEF, %	91	88	83	81

Underlined values are statistically significantly different between fast- and slow-conducting pyramidal tract projecting neurons (PTNs) according to Student's unpaired t test for averages (means \pm SE) or according to the Z test for proportions. dM, depth of modulation; KA, kainic acid; M, coefficient of stride-related frequency modulation defined as $M = (F_{\min}/F_{\max})100\%$, where F_{\min} and F_{\max} are the mini-mal and the maximal frequencies of discharge in the histogram; PEF, period of elevated firing; RF, receptive field; VL, ventrolateral thalamus. Bold type indicates statistical significance: **values** that are statistically significantly greater during flat surface locomotion than during standing; **values** that are statistically significantly greater during ladder locomotion than flat surface locomotion; **values** that are statistically significantly smaller after KA lesions in the VL than before the lesions. The coefficient of variability of discharge rate, CV, was defined as $CV = s/m$, where s is standard deviation and m is mean firing rate.

The hallmark of this new response was a uniform increase of the discharge rate throughout the step cycle (by 4 spikes/s; $P = 0.051$, t test; Fig. 10, C4 and D4) rather than an activity increase during stance observed in normal conditions (Fig. 10, A4 and B4). About two-thirds of neurons (72%, 47/65) changed their discharge rate: 46% (30/65) increased by 12.7 ± 10.5 spikes/s and 26% (17/65) decreased by 6.2 ± 3.2 spikes/s (Fig. 11D). Although the proportions of neurons changing the discharge rate were similar to those in normal conditions (Fig. 11A; APPENDIX A), the values of the change were not. Neurons that decreased activity did so less on average ($P = 0.001$, t test). In result, the discharge rate of the population during ladder locomotion was similar to that before the lesions (18.6 ± 13.4 and 21.0 ± 12.5 spikes/s, respectively; $P > 0.05$, t test). The dM changed in 63% of the neurons, which was also a similar proportion to that seen in normal conditions (Fig. 11, B and E; APPENDIX A). However, the dM also changed differently compared with normal. Significantly fewer neurons increased the dM (23%, 15/65), whereas more neurons decreased it (40%, 26/65) ($P = 0.024$ and $P = 0.032$, respectively, Z test). The proportion of neurons shifting the preferred phase was similar to that in normal conditions ($P > 0.05$, Z test; Fig. 11, C and F; APPENDIX A). These phase shifts made the population recruitment steadier across the step cycle because more neurons were active

during the stance phase during locomotion on the ladder (Fig. 10, C3 and D3). We will argue in the DISCUSSION that these changes, particularly the normal average discharge rate and possibly the alteration of the mode of activity modulation, contributed to the success of ladder locomotion.

Reorganization of the activity of motor cortex populations related to the shoulder, elbow, and wrist/paw.

Neurons with somatosensory RFs on different segments of the forelimb, thus likely controlling different segments of the forelimb, coped differently with lesions in the VL. During locomotion on the flat surface, the shoulder- and wrist-related groups lost 6.9 spikes/s and 9.2 spikes/s in the average discharge rate, respectively ($P = 0.028$ and $P = 0.05$, correspondingly, t test), representing 33% and 40% decreases in their activity compared with normal conditions. In contrast, the elbow-related group retained its discharge rate. The activity profiles were still different among the groups. The elbow- and wrist/paw-related population profiles, albeit less prominent, roughly resembled the normal ones (Fig. 12, B1, B2 and C1, C2), whereas the profile of the shoulder-related group changed from one with a peak during stance to one with a peak during swing (Fig. 12, A1 and A2).

All groups responded differently to the demand for movement accuracy on the ladder after the VL was lesioned. The shoulder-related group increased its activity during the swing rather than stance phase ($P = 0.001$, U test; Fig. 12, A2 and A4), the elbow-related group did not show any response (Fig. 12, B2 and B4), and the wrist/paw-related group uniformly increased its activity throughout the step cycle ($P < 0.001$, U test; Fig. 12, C2 and C4). Remarkably, the average discharge rates of all groups during ladder locomotion were

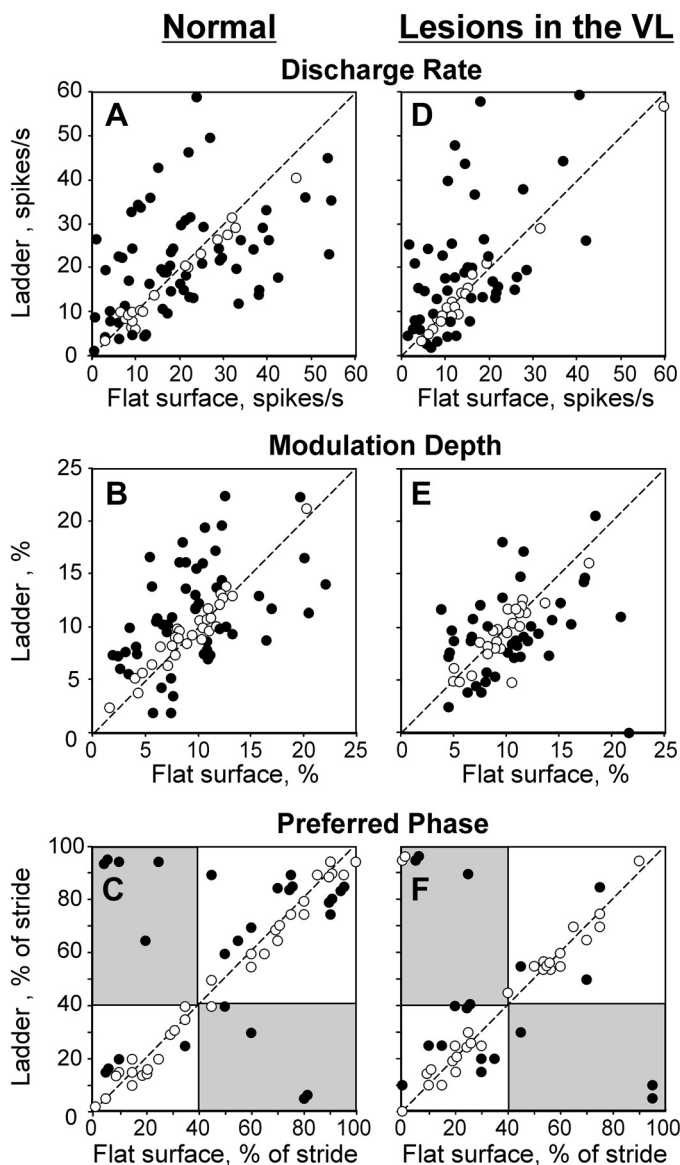


Figure 11. Responses of individual neurons to the ladder task in normal conditions (left three) and after lesions in the ventrolateral thalamus (VL) (right three). The abscissa and ordinate of each point show the values observed during flat surface and ladder locomotion, respectively. Neurons with characteristics that were statistically significantly different between the two locomotion tasks (see METHODS) are shown with filled circles; the others are shown with open circles. A and D: mean discharge frequency averaged over the stride. B and E: depth of frequency modulation, dM. C and F: preferred phase of activity for neurons with a single period of elevated firing (PEF) during both locomotion tasks. Areas that correspond to the swing phase during one task but the stance phase during the other task are shaded. Other designations are as in Fig. 5.

similar to those in normal conditions ($P > 0.05$, t test). However, the distributions of the activity across the step cycle were different, especially in the shoulder-related group. As we will discuss in the DISCUSSION section, these changes, particularly the re-focusing of the activity on the swing phase by the shoulder-related group and the increase of the overall output by the wrist/paw-related group must have contributed to the success of ladder locomotion.

Reorganization of the activity of motor cortex efferent populations after lesions in the VL.

All three studied groups of motor cortical efferent neurons responded to lesions in the VL, but they did so differently. On the flat surface, the average discharge rate of the fast-conducting PTNs decreased by 29% ($P = 0.036$, t test; Table 3), with the most prominent decrease occurring during the first half of swing and the second half of stance (Fig. 12, D1 and D2). In result, the fast-conducting PTNs became most active during swing and the swing-to-stance transition rather than the stance-to-swing transition. Switching to the ladder task, the discharge rate of this group tended to increase and was now similar to normal (Fig. 12, D2 and D4; Table 3). The activity increased most during swing (Fig. 12, D2 and D4), while remaining lower than normal during stance (Fig. 12, D3 and D4). This was different from how fast-conducting PTNs responded to the ladder task in normal conditions when their firing increased during stance rather than swing (Fig. 12, D1 and D3; see also data for a larger population in Ref. 50). In addition, the average depth of modulation (both the dM and M indexes) diminished in this group, whereas the discharge variability (CV) increased on the ladder when the VL was lesioned (Table 3).

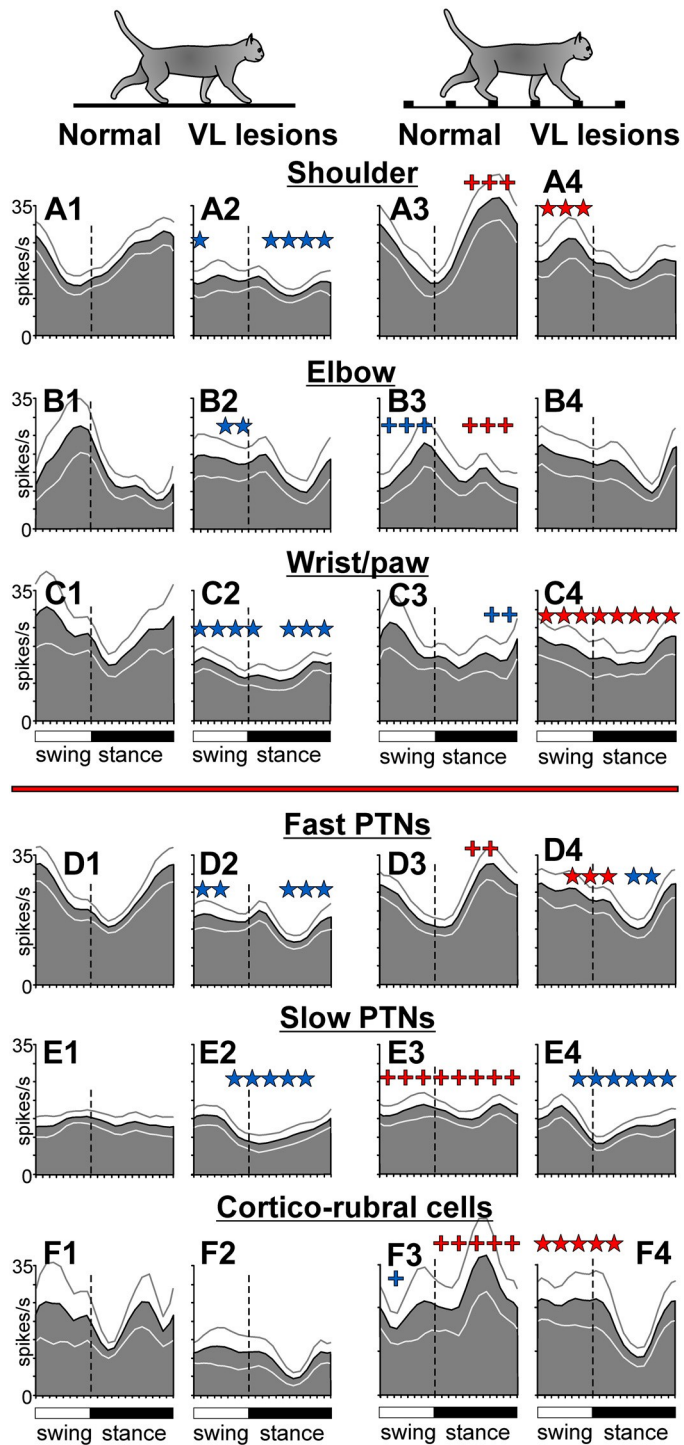
In contrast to fast-conducting PTNs, the discharge rate of the slow-conducting PTNs during either locomotion task did not change after lesions in the VL ($P > 0.05$, t test; Table 3). Similarly to fast-conducting PTNs, their activity peaked in the swing phase of the stride during both locomotion tasks (Fig. 12, E2 and E4). This was different from the normal activity profiles of this group, in which the activity was evenly distributed across the step cycle (Fig. 12, E1 and E3).

The average activity of the cortico-rubral cell group during flat surface locomotion was similar to that in normal conditions. However, the activity pattern was altered as the activity dip during stance occurred later in stance (Fig. 12, F1 and F2). The response of the cortico-rubral group to the ladder task was also different from normal as its activity vigorously increased during swing while barely changing in the middle of stance ($P < 0.001$, U test; Fig. 12, F2 and F4 vs. F1 and F3).

DISCUSSION

In this study, we investigated neuronal mechanisms of reorganization of motor cortex activity during locomotion after temporary inactivation and permanent lesion in a part of the VL. Behaviorally, we found that a 2–4 h inactivation of 10% of the VL unilaterally had only a very minor effect on locomotion on either the flat or complex surface, and that more severe locomotor deficits observed on the complex

surface after a lesion of 50%–75% of the VL bilaterally were compensated in a few days. However, the locomotion-related activity of the motor cortex substantially changed both during the temporary inactivation and after the permanent lesions in the VL. After both interventions, the average discharge rate during locomotion on the flat surface was reduced by 30%, and it was similarly reduced during ladder locomotion after temporary inactivation but not after the permanent lesion. There was also a substantial reorganization of the activity



patterns of individual neurons and neuronal subpopulations after both interventions. We suggest that this reorganization of neuronal activity contributed to the maintenance of successful locomotion on the complex surface during temporary inactivation in the VL and to the recovery of locomotion after permanent lesions in the VL.

Reorganization of Motor Cortex Activity during Locomotion on the Flat Surface

During locomotion on the flat surface after temporary inactivation or permanent lesion in part of the VL, the discharge rate of motor cortex neurons was substantially reduced, particularly during the swing phase and second half of stance (Fig. 4C4 vs. Fig. 4A4 and Fig. 10C4 vs. Fig. 4A4). In addition, after the lesion, the recruitment of neurons during stance was reduced (Fig. 10C3). Despite these changes, the discharge rate of nearly every individual neuron was still modulated with the locomotor rhythm after both interventions, showing the same depth of modulation and the same number of PEFs of the same duration as in normal conditions (Figs. 5 and 11, Table 3). Also, the activity profiles of all neuronal subpopulations were still modulated with the rhythm, although some had a reduced peak-to-peak range (Figs. 8 and 12). In addition, the elbow-related group maintained its overall discharge rate fairly well after both interventions (Fig. 8, B1 and B2 and Fig. 12, B1 and B2), and the wrist/paw-related group held it during temporary VL inactivation (Fig. 8, C1 and C2). Regarding different cortical efferent systems after the permanent lesion, the peak activity of both the fast- and slow-conducting PTN populations shifted toward the swing phase of the stride (Fig. 12, D and E). The slow-conducting PTNs, which in normal conditions are substantially less active than the fast-conducting PTNs (Table 3; see also Ref. 50), maintained their activity fairly well both during temporary inactivation and after the permanent lesion in the VL. Thus, the elbow- and wrist/paw-related cell groups and the slow-conducting PTNs contributed the most to the maintenance of motor cortex population activity after a malfunction in the VL.

Was this activity reorganization in the motor cortex necessary for successful locomotion on the flat surface after

Figure 12. Phase distributions of average discharge frequencies of groups of neurons with somatosensory receptive fields (RFs) on different segments of the forelimb, as well as those of neurons with different destinations of the axon and axonal conduction velocity. Data for flat surface locomotion (left two columns) and ladder locomotion (right two columns) in normal conditions and after kainic acid (KA)-induced lesions in the ventrolateral thalamus (VL) are shown. A: activity of neurons responsive to passive movement in the shoulder joint or tactile stimulation of the shoulder in normal conditions (A1 and A3; $n = 22$) and after lesions in the VL (A2 and A4; $n = 26$). B: activity of neurons responsive to passive movement in the elbow joint or palpation of arm muscles (12 cells tested in normal conditions, 15 tested after lesions in the VL). C: activity of neurons responsive to passive movement in the wrist joint or tactile or deep tissue stimulation of the paw (18 cells tested in normal conditions, 18 tested after lesions in the VL). D: activity of fast-conducting pyramidal tract projecting neurons (PTNs) (47 cells tested in normal conditions, 34 tested after KA-induced lesions in the VL). E: activity of slow-conducting PTNs (25 cells tested in normal conditions, 21 tested after lesions in the VL). F: activity of PTNs and other neurons projecting to the red nucleus (8 cells tested in normal conditions, 12 tested after lesions in the VL). Other designations are as in Fig. 8.

inactivation or lesion in the VL? It probably was not. It was previously found that the activity of the motor cortex is not needed for cats to walk successfully on the flat surface (32–34, 38). The neural mechanism that determines the order of muscular contractions and the coordination of limbs during locomotion on the flat surface resides in the spinal cord (114–117), and body posture is maintained by the activity of the brainstem and cerebellum (118–121). It is only when the animal encounters a complex surface on which locomotor movements need to be adjusted to avoid obstacles or step accurately on specific sites that the motor cortex and motor thalamus become involved. We previously suggested that the stride-related modulation of the activity of the motor cortex on the flat surface has an informational, preparatory function. It creates a structured frame for the activity that can be used during locomotion on a complex surface to convey corrective signals to subcortical centers and the spinal cord in just the right phases of the stride so that the function of these centers is not disrupted while being adjusted (11, 34, 80). Such “right” phases are hypothesized to be identified by the preferred phases of the activity of individual neurons and the periods of elevated activity of specific neuronal subpopulations. During these phases, cortical signal transmission is enhanced.

How did this guiding frame reorganize after lesions in the VL? At the population level, barring a few exceptions, the reorganization can be summarized as follows. The frame became less salient in both the absolute firing rates and peak-to-peak discharge ranges defining it. In addition, for some subpopulations, the periods of elevated transmission shifted toward the swing phase of the stride. In half of individual neurons, however, the depth of the stride-related activity modulation increased, which may have partly compensated at the level of single neurons for the reduction of the silence of the population-based activity frame.

Reorganization of Motor Cortex Activity for Accurate Stepping on the Complex Surface

The activity of the motor cortex is necessary for successful locomotion on the complex surface (32–39). Both humans and cats adjust strides to the complexities of the surface based chiefly on visual information about it (e.g., Refs. 122–124). Motor cortex is one of the sites where the final integration of visual and movement-related information occurs during locomotion before the cortical signal for step adjustment is dispatched to subcortical centers and the spinal cord (for review, see Ref. 125). Upon transition from locomotion on the flat surface to stepping accurately over obstacles or along a horizontally placed ladder, the activity of the overwhelming majority of neurons in the motor cortex changes (34, 44–46, 49–52, 59, 80). The discharge rate of neurons either increases or decreases (e.g., Fig. 5A and Fig. 11A), the depth of modulation typically increases but can also decrease (e.g., Fig. 5B and Fig. 11B), and the duration of the activity burst often decreases, making the burst more stride-phase specific. Because the pattern and PrPh of the activity change much less frequently than the discharge rate and depth of modulation (e.g., Figs. 5 and 11), one can consider that in normal conditions, the guiding frame for adjustment of steps to the complex surface described earlier is typically used.

Reorganization during a short-lasting inactivation in the VL.

When part of the VL was temporarily inactivated and the thalamo-cortical signal was reduced, neurons in the motor cortex still responded to the need to make steps accurately on the ladder, and locomotion was successful. Both the overall proportion of responding neurons and the proportions of neurons responding by increasing or decreasing the value of each tested activity parameter were normal (Fig. 5). This ensured that, although the input from the VL was compromised, the same number of cortical signals of each kind—that is, an increase or decrease of a neuron’s discharge rate and depth of modulation—was still sent to subcortical centers and the spinal cord. The changes in activity upon transition from the flat surface to the ladder presumably convey vision information-based directives for step adjustment on the ladder. Since the preferred phases of the activity and the duration of PEFs often did not change with the transition from the flat surface to the ladder (Fig. 5F), one can conclude that the guiding frame for signals for steps adjustment that operated in normal conditions was still used during inactivation in the VL despite being less salient. Moreover, similar to locomotion on the flat surface, during ladder locomotion, the depth of activity modulation of individual neurons was often higher after inactivation in the VL than normal. This may represent a component of the compensation mechanism that increased the salience of the signal at the level of individual neurons, helping locomotion on the ladder to be successful. We have previously suggested that a change, most often an increase, in the depth of modulation of individual neurons represents a signal for adaptation of locomotor movements to complexities of the surface (34, 80). That ladder locomotion was successful despite specific bits of this information were conveyed by different sets of neurons implies that during the short-lasting inactivation in a part of the VL, it is not as important for control of accurate stepping which particular neurons of the motor cortex convey the results of cortical processing to subcortical centers and the spinal cord as is the total number of such neurons transmitting the signal. This can be compared with a choir, where it does not matter who sings a particular part as long as all parts are sung.

The normal proportions of neurons responding to the demands of the ladder task in the face of inactivation in the VL can probably be explained by the highly divergent and also convergent nature of the thalamo-cortical projection in the motor system (126). This projection is organized such that each small area of the VL projects to a wide area of the motor cortex, and each small area of the motor cortex receives inputs from a wide VL area. With such a projection, even when 50%–75% of the VL is damaged, each area of the motor cortex receives the signal, albeit at a lower intensity.

For nearly every neuron, the change in the discharge rate after inactivation in the VL was not uniform across the step cycle but varied, typically alternating between an increase and decrease (78). We identified six groups of neurons: cells that mostly lose activity, those that mostly gain it, and neurons that lose activity during some phases of the stride while gaining it during other phases (Supplemental Fig. S1).

For the stability of the activity pattern of the motor cortex layer V population after an inactivation in the VL, it was certainly beneficial that different neurons lost their activity during different phases of the stride, and some even gained it. Thereby, although the average discharge rate of the entire population was diminished, the population's activity pattern remained largely unchanged (Fig. 4).

Reorganization after a permanent lesion in the VL.

After the permanent lesion of large VL areas, the overall proportions of neurons responding to the demands of the ladder task with a change in the discharge rate or depth of activity modulation were also similar to those observed in normal conditions (Fig. 11). However, unlike during the temporary inactivation of a smaller VL area, the prevailing type of response was now an increase of the (depressed) discharge rate and a decrease of modulation depth. For the swing phase of the stride, where the activity of all groups of efferent neurons concentrated after the lesion (Fig. 12, D4–F4), the increase in the discharge rate was sufficient to bring the population's activity to the normal level; however, this was not the case for the stance phase, where the activity remained lower than normal (Fig. 10D4 vs. Fig. 10B4). Nevertheless, unlike during temporary VL inactivation, when the population's discharge rate during ladder locomotion was lower than normal, 1–4 wk after the permanent VL lesion, the discharge rate during ladder locomotion was normal. We suggest that this was the major component of the recovery of motor cortex activity that contributed to the success of ladder locomotion after the lesion. In an early study in which we lesioned the VL electrolytically, we also saw that motor cortex neurons chiefly responded to the demands of the ladder task after the lesion by increasing their overall discharge rate (11).

Shifting the focus of the activity toward the swing phase of the stride for stepping on the ladder could also have been beneficial for the successful visuomotor coordination on the ladder because this is the phase during which cats fixate gaze on the crosspiece where the limb will land in the next stride and likely collect visual information about the cross-piece's location (124, 127). The horizontal position of the paw during the initial and terminal swing phase of the stride on the ladder is then actively stabilized (128). Thus, the greater than normal increase of the activity during the swing phase upon transition from the flat surface to the ladder could be a cortical mechanism for compensation for the lost VL signal. For humans, whose locomotion biomechanics necessitate the collection of visual information for the next step on complex terrain during the preceding stance rather than swing (122, 123, 129), it could be beneficial to increase cortical activity during stance.

Regarding the decrease in the depth of activity modulation, which was more often observed upon the transition from flat surface to ladder locomotion after the VL lesion than in normal conditions, we suggest that it was a tool for control of accurate stepping after the lesion. Such a tool is used by about a quarter of motor cortex neurons, even in normal conditions (34, 49, 50, 80). Moreover, the decrease in the modulation depth is the preferred response of motor cortex neurons while adjusting steps during locomotion along a narrow flat strip where the left-right rather than forward-backward accuracy of movements is required (52). In addition, like what was observed in

this study after the VL lesion, during adaptation to locomotion on the narrow surface, the reduction of the depth of modulation is paired with an increase in the discharge rate.

Role of the motor cortex in the recovery and maintenance of locomotion.

Was the reorganization of the activity in the motor cortex during the temporary inactivation and after permanent lesions in the VL responsible for the maintenance and recovery of successful locomotion on the ladder? We believe that it was, at least in part. We argue that the fact that normal proportions of motor cortex neurons responded to the ladder task after both the temporary inactivation and permanent lesion in the VL (Figs. 5 and 11), albeit in an altered manner, indicate that the motor cortex did contribute to the success of ladder locomotion after interventions in the VL. This is likely so because the results of studies of motor cortex activity, particularly the devastating effects of the activity blockade on performance of skilled locomotion, indicate that changes in the motor cortex activity upon transition from flat to uneven surface represent commands for the adjustment of steps to the surface (11, 32–35, 37–39, 44, 45, 52, 59, 61, 80). In addition, the fact that after the permanent lesion in part of the VL, the discharge rate during flat surface locomotion—a task for which the activity of the motor cortex is not needed—was much lower than normal, but it was normal during ladder locomotion—the task that requires motor cortex activity to be successful—is striking. Furthermore, it seems that the motor cortex was switching to different control strategies during the temporary inactivation and after the permanent lesion in the VL. Namely, during the small and short-lasting VL inactivation, the strategy was to regroup neurons in such a way as to still send the normal number of signals of each kind to the downstream centers, whereas for the recovery from a large permanent lesion, the strategy was to increase the overall volume of the signal and decrease its step-phase modulation in individual neurons. Since locomotion was successful after each of the VL malfunctions and the associated reorganization of the activity in the motor cortex, we believe that the observed reorganization contributed, at least in part, to the recovery and maintenance of successful locomotion on the ladder when the VL malfunctioned. PET and fMRI studies of thalamic stroke survivors and patients with thalamotomy showed too that the recovery after a subcortical lesion positively correlates with the restoration of normal activity in the motor cortex (62–67, 76). An essential role of the motor cortex in learning a nondexterous motor skill has also been demonstrated in rats (130).

Contribution of different neuronal subpopulations to reorganization and recovery.

Both during the temporary inactivation and after permanent lesions in the VL groups of neurons with somatosensory RFs on different segments of the forelimb, i.e., groups that are believed to control movement of different limb segments, differed in their contribution to the reorganization of motor cortex activity. During the temporary inactivation in the VL, the wrist-related group fully retained its response to the ladder task, whereas the response of the elbow-related group was only partly preserved, and the shoulder-related group

lost its response (Fig. 8). In the motor cortex, there is a fair correspondence between where on the body the somatosensory RF of a neuron is located and which part of the body the activity of this neuron influences (86–88, 99). Thus, the observation that the wrist-related group maintained its normal response to the ladder task in the face of inactivation in the VL suggests that this group was still contributing normally to the performance of this task while the VL malfunctioned. This is important for successful locomotion on the ladder because the wrist orients the paw so that it lands accurately on crosspieces (80). A prominent activity peak of the elbow-related group during the transition from the swing to stance phase of the stride, which was similar to that seen in normal conditions (Fig. 8, B2 and B4), must have contributed to the normal movement of the elbow and the success of ladder locomotion during inactivation in the VL.

The situation differed after the permanent lesion in the VL. During locomotion on the ladder, discharge rates of all groups of neurons, including the shoulder-related group, were close to normal. However, while the activity profiles of the wrist/paw- and elbow-related groups were close to normal, the profile of the shoulder-related group changed (Fig. 12). That the activity profile of the shoulder-related group during ladder locomotion switched from one with a peak during the stance phase before the lesion to one with a peak during the swing phase after the lesion suggests that when ladder locomotion recovered after the lesion, the shoulder was controlled differently from normal. This is an important finding because in normal conditions, most of the movement adjustment during locomotion on the ladder is produced by the shoulder, particularly at the end of the swing phase when an active muscle torque is generated at the shoulder and influences movement of the entire limb (131). The post-VL lesion reorganization of motor cortex activity appears to have been directed toward an increase of the control over the shoulder during the swing phase of the stride.

Both during the temporary inactivation and after the permanent lesion in the VL neurons with different destinations and properties of the axon: PTNs with axons conducting with different velocities, cortico-rubral cells, and neurons whose projections were not identified, noIDs, contributed differently to the reorganization of motor cortex activity for support of successful accurate stepping on the ladder. The slow-conducting PTNs contributed substantially as during the temporary inactivation, they increased their overall discharge rate, and after both interventions, they adjusted the discharge pattern so that more activity occurred during the swing than stance phase of the stride (Fig. 8E and Fig. 12E). We previously found that in normal conditions, the slow-conducting PTNs respond to the demands of the ladder task in a much more concerted manner than the fast-conducting PTNs do by increasing their discharge rate and its stride-related modulation and decreasing discharge variability (50). Thus, we suggested that slow-conducting PTNs are involved in controlling the accuracy of locomotor movements to a greater degree than fast-conducting PTNs are (50). Here, we showed that they also contribute substantially to the maintenance of motor cortex activity during a malfunction in the VL.

That the average discharge rate of fast-conducting PTNs was retained during inactivation in the VL suggests that this group also contributed to the success of ladder locomotion

in this condition by supporting the average intensity of the motor cortical signal to the subcortical centers and the spinal cord. The fact that the cortico-rubral cells, most of which were also fast-conducting PTNs, largely maintained their average discharge rate after permanent lesions in the VL suggests that the normal intensity of the signal to the red nucleus, which is an important subcortical motor center and the source of the major brainstem-spinal cord descending tract, was important for the recovery of successful locomotion on the ladder after the lesions.

Unlike efferent neurons, which maintained their average discharge rates close to normal during locomotion on the ladder, despite the temporary inactivation or permanent lesion in the VL (Fig. 8, D and E and Fig. 12, D–F), the group of noID neurons tended to lose activity, and during temporary inactivation, they lost their discharge pattern (Fig. 8F). Many of the noIDs in this sample are likely to have been interneurons. Thus, the fact that the response of noIDs to the ladder task suffered more than that of PTNs suggests that mechanisms may have been engaged to preferentially support the activity of efferent populations, which convey the output of the motor cortex to other motor centers and the spinal cord, so that the larger locomotor network's functionality is maintained rather than simply preserving the activity of every neuron in the motor cortex.

Translational Perspective

Diaschisis, the multifaceted change in brain areas remote from the area of stroke, has been recognized for over 100 years (132–134). To aid recovery and rehabilitation after stroke, one needs to know what neurons and neuronal connections have suffered not only in the area directly affected by the stroke but also in the areas that would normally receive inputs from the area of stroke and now have lost their inputs, as well as those that were previously projecting to the area of stroke and now have lost their targets. A significant portion of disabilities after stroke results not from the loss of nervous tissue in the area of stroke but from malfunction of many other regions of the nervous system that suffer from the loss of their connections with the area of stroke. These disabilities range from dysfunctions of systems supporting basic body functions to mood disorders. After stroke, the affected neurons distributed throughout the nervous system need to be assisted in their normal function. Were we able to do this, the clinical consequences of strokes would be significantly reduced.

In this study, we analyzed reorganization of neuronal activity in the motor cortex during a temporary inactivation and after a permanent lesion in the VL, the reorganization that apparently supported successful locomotion on the complex surface despite a significant malfunction in the thalamus. A better understanding of the mechanisms of spontaneous recovery may provide useful guidance for the development of new clinical approaches to assist poststroke recovery. Extending the old concept of diaschisis and paving a new avenue for related research, we investigated the spiking activity of single neurons and several identified neuronal subpopulations in the motor cortex as animals coped with or recovered from a malfunction in the thalamus. Many studies have investigated changes in the global characteristics of motor cortex activity after a thalamic lesion, such as EEG and metabolic changes, and the reorganization of cortical "motor maps" revealed by

cortical stimulation (e.g., see Refs. 62–70). The subcellular events, such as reorganization of synapses and synaptic plasticity in the motor cortex after a lesion in the ventrolateral thalamus, were also studied to some extent (e.g., see Refs. 71–75). However, the electrical activity of single neurons and specific subpopulations of neurons in motor cortex after thalamic stroke or lesion was not previously researched, except for one study by Sidorov (77) conducted in anesthetized animals. The need in this knowledge for the development of new rehabilitation approaches is rapidly growing as methods for targeted modulation of the activity of single neurons and specific neuronal populations are expected to become available.

The results of our study suggest that even a stride-phase imprecise “blurred” activation of arbitrarily selected motor cortical efferent neurons, if done according to a natural activity pattern, may reduce or even eliminate ataxia during locomotion. The results suggest that for the recovery of successful locomotion on a complex natural terrain, it may be beneficial to focus rehabilitative efforts on activation of the proximal–hip-related—neuronal networks in the motor cortex. We hope that the information obtained in this study will be useful for the development of new rehabilitation approaches for patients with thalamic stroke or lesion, approaches that would assist the function of the motor cortex at the level of single neurons and specific subpopulations of neurons.

APPENDIX A: ACTIVITY OF MOTOR CORTEX NEURONAL POPULATIONS OF CAT A IN NORMAL CONDITIONS

As previously found for the activity of layer V motor cortex neurons in cats (11, 34, 44, 45, 49, 50, 80), the activity of 94% (77/81) of cat A neurons during locomotion on the flat surface was modulated with the rhythm. PEFs were distributed over the step cycle so that 50%–70% of neurons were active in every stride phase (Fig. 10, A1 and A3). Neurons with PEFs during the transition from stance to swing were more active than those with PEFs during the transition from swing to stance (Fig. 10A2), which resulted in the activity of the entire population being higher during the stance-to-swing transition phase than in the beginning of the stance phase ($P = 0.001$, U test; Fig. 10A4). Upon switching to ladder locomotion, three-quarters of neurons changed their average discharge rate: 40% (32/81) increased by 12.8 ± 10.9 spikes/s, while 37% (30/81) decreased by 10.3 ± 7.5 spikes/s on average (Fig. 11A). In addition, the dM changed in 64% of neurons, increasing in 41% (33/81), and decreasing in 23% (19/81; Fig. 11B). The PrPh of a few neurons shifted to stance (Fig. 11C), and neurons with PEFs during stance became more active (Fig. 10B2). In result, the activity of the population increased during the mid-stance phase of ladder locomotion ($P = 0.031$, U test; Fig. 10B4).

Groups of neurons with somatosensory RFs associated with different segments of the forelimb were preferentially active during different phases of the stride. On the flat surface, the shoulder-related group was most active at the end of stance (Fig. 12A1), the elbow-related group was mainly active at the end of swing (Fig. 12B1), and the wrist/paw-related group was most active in the beginning of swing (Fig. 12C1). Upon transition to the ladder, the shoulder-related group further increased its activity during the end of stance ($P = 0.003$, U test; Fig.

12A3), the elbow-related group developed an additional activity peak in the middle of stance ($P = 0.007$, U test) and reduced the activity during swing ($P = 0.048$, U test; Fig. 12B3), whereas the wrist/paw-related group reduced the activity at the end of stance ($P = 0.012$, U test), making the activity peak in the beginning of swing more prominent (Fig. 12C3). These activity changes were consistent with our previous observations in a larger population of motor cortex neurons (49).

The fast-conducting PTN group was almost twice as active as the slow-conducting PTN group ($P = 0.004$, t test), and its activity was more modulated (Fig. 12, D1 and E1). Upon transition to ladder locomotion, the activity of the slow-conducting PTNs increased by 20% throughout the step cycle ($P < 0.001$, t test) and became modulated (Fig. 12, E1 and E3), whereas the activity of fast-conducting PTNs increased during the middle of stance only ($P = 0.03$, U test; Fig. 12, D1 and D3) while remaining sharply modulated. These activities are consistent with our previous report on a larger neuronal population (50). The activity of the group of cortico-rubral neurons, most of which were fast-conducting PTNs, was largely similar to that of the fast-conducting PTN group during flat surface locomotion; however, unlike that group, the cortico-rubral cells responded prominently to the ladder task by increasing their activity during the stance phase of the step cycle and decreasing it during swing ($P < 0.001$ and $P = 0.012$, respectively, U test; Fig. 12, F1 and F3).

APPENDIX B: DETAILS OF KA LESIONS IN THE THALAMUS OF CAT A

Left Side

The left hemibrain was sliced parasagittally, and we describe the lesion as appearing in sections going from medial to lateral. Medially, the lesion started at L2.5 right outside the VL as a circle of 1.5 mm in diameter. By L3.0, it grew to 2 mm in diameter, now covering most of the VL but not touching other nuclei in any significant way. The lesion remained this way until L4.0, where it expanded ventrocaudally to include a small part of the nucleus ventralis posteromedialis (VPM), ventro-rostrally to consume 2 mm of the reticular nucleus of thalamus (RE) and also dorsorostrally to include some of the nucleus ventralis anterior (VA). The zona incerta (ZI) and nucleus centralis lateralis (CL) remained intact. At L4.5, the lesion expanded still more rostrally, now consuming all the rostral RE yet sparing a significant part of the VA (1.51 mm, encircled in Fig. 9B). The ZI and CL were still intact, and the VPM was only slightly touched. By L5.0, the VA was fully included in the lesion, and part of the nucleus dorsalis lateralis (LD) above the VL was damaged by the guide tubes.

At L5.3, the lesion began to recede, freeing a part of the VA and a 1 mm wide strip in the ventrocaudal part of the VL (Fig. 9C). At this level, however, the lesion started damaging the rostral part of the nucleus ventralis posterolateralis (VPL) that emerged below and caudally to the VL. The lesion continued in this manner until L6.5, where it broke into two areas: the rostral one, which included the RE and a part of VA, and the caudal one, which included the ventrocaudal part of the VL and was touching the VPL (Fig. 9D). The lesion rapidly diminished after L6.5, first vacating the VA, then the

VL, and finally the RE, and it disappeared by L7.0. The atlas by Reinoso-Suarez (104) does not show the VL at laterality greater than 7.0. However, the atlas of Berman and Jones (135) shows the VL up to 7.5.

Right Side

The right hemibrain was sliced frontally, and we describe the lesion as it appears in the sections going from caudal to frontal. Caudally, the lesion started at A7.5, where the laminar structure of the lateral geniculate nucleus was still visible. The lesion was located right behind the VL. By A8.0, the lesion encompassed most of the VL, which is small at this level; the very top of the VPM; and a small part of the bottom of the nucleus lateralis posterior (LP; Fig. 9F). At A8.5, the lesion still covered much of the VL, plus it expanded ventrally to include about one-third of the VPM. At A9.0, one-third of the VPM was damaged along with about one-quarter of the LP, while the medial half of the VL and all the VPL remained intact (Fig. 9G). At 9.5, where the VPL expands medially to replace the VPM, about half of each VL and VPL was damaged, as well as about one-third of the LP. At 10.0, only the lateral one-quarter to one-third of the VL was lesioned, whereas about half of each of the VPL and LP was damaged (Fig. 9H). The lesion abruptly ended at A10.5, where only a small middle part of the VL was lesioned. The VL is still recognized at A11.0, where it was all intact.

SUPPLEMENTAL DATA

Supplemental Fig. S1: <https://doi.org/10.6084/m9.figshare.16441869>.

DATA AVAILABILITY

Raw and processed data are available through the cat-brain.org open database.

ACKNOWLEDGMENTS

The author thanks Dr. Zinaida Tamarova for conducting a part of experiments with cat A and Dr. Vladimir Marlinski for conducting experiments with cat B, a part of initial data analyses, and construction of Figs. 1A, 3, and 6. The author is indebted to Peter Wettenstein for exceptional engineering assistance.

GRANTS

This work was supported by the National Institute of Neurological Disorders and Stroke at the National Institutes of Health Grant R01 NS-058659 (to I. N. Beloozerova) and by the National Science Foundation Grant 1912557 (to I. N. Beloozerova).

DISCLOSURES

No conflicts of interest, financial or otherwise, are declared by the author.

AUTHOR CONTRIBUTIONS

I.N.B. conceived and designed research; performed experiments; analyzed data; interpreted results of experiments; prepared figures; drafted manuscript; edited and revised manuscript; approved final version of manuscript.

ENDNOTE

At the request of the author, readers are herein alerted to the fact that additional materials related to this manuscript may be found at cat-brain.org. These materials are not a part of this manuscript and have not undergone peer review by the American Physiological Society (APS). APS and the journal editors take no responsibility for these materials, for the website address, or for any links to or from it.

REFERENCES

1. Garcin R. Syndrome cerebellothalami par lesion localisee du thalamus. *Rev Neurol (Paris)* 93: 143–149, 1955.
2. Bogousslavsky J, Regli F, Uske A. Thalamic infarcts: clinical syndromes, etiology, and prognosis. *Neurology* 38: 837–848, 1988 [Erratum in *Neurology* 38: 1335, 1988]. doi:[10.1212/WNL.38.6.837](https://doi.org/10.1212/WNL.38.6.837).
3. Melo TP, Bogousslavsky J, Moulin T, Nader J, Regli F. Thalamic ataxia. *J Neurol* 239: 331–337, 1992. doi:[10.1007/BF00867590](https://doi.org/10.1007/BF00867590).
4. Solomon DH, Barohn RJ, Bazan C, Grissom J. The thalamic ataxia syndrome. *Neurology* 44: 810–814, 1994. doi:[10.1212/WNL.44.5.810](https://doi.org/10.1212/WNL.44.5.810).
5. Gupta N, Pandey S. Postthalamic stroke movement disorders: a systematic review. *Eur Neurol* 79: 303–314, 2018. doi:[10.1159/000490070](https://doi.org/10.1159/000490070).
6. Jeljeli M, Strazielle C, Caston J, Lalonde R. Effects of ventrolateral-ventromedial thalamic lesions on motor coordination and spatial orientation in rats. *Neurosci Res* 47: 309–316, 2003. doi:[10.1016/s0168-0102\(03\)00224-4](https://doi.org/10.1016/s0168-0102(03)00224-4).
7. Fabre M, Buser P. Structures involved in acquisition and performance of visually guided movements in the cat. *Acta Neurobiol Exp (Wars)* 40: 95–116, 1980.
8. Cherenkova LV, Yunatov IA. [Participation of the ventrolateral thalamic nucleus in organizing visually controlled movements in the cat]. *Zh Vyssh Nerv Deiat Im IP Pavlova* 33: 472–479, 1983.
9. Batuev AS, Cherenkova LV, Yunatov YA. Association brain systems and visually guided movements in the cat. *Physiol Behav* 31: 29–38, 1983. doi:[10.1016/0031-9384\(83\)90092-6](https://doi.org/10.1016/0031-9384(83)90092-6).
10. Fabre-Thorpe M, Levesque F. Visuomotor relearning after brain damage crucially depends on the integrity of the ventrolateral thalamic nucleus. *Behav Neurosci* 105: 176–192, 1991. doi:[10.1037/0735-7044.105.1.176](https://doi.org/10.1037/0735-7044.105.1.176).
11. Beloozerova IN, Sirota MG. The role of motor cortex in control of locomotion. In: *Stance and Motion. Facts and Concepts*, edited by Gurfinkel VS, Ioffe ME, Massion J, Roll JP. New York: Plenum Press, 1988, p. 163–176.
12. Beloozerova IN, Sirota MG. Cortically controlled gait adjustments in the cat. *Ann N Y Acad Sci* 860: 550–553, 1998. doi:[10.1111/j.1749-6632.1998.tb09101.x](https://doi.org/10.1111/j.1749-6632.1998.tb09101.x).
13. Carrera E, Bogousslavsky J. The thalamus and behavior: effects of anatomically distinct strokes. *Neurology* 66: 1817–1823, 2006. doi:[10.1212/01.wnl.0000219679.95223.4c](https://doi.org/10.1212/01.wnl.0000219679.95223.4c).
14. Massion J. The thalamus in the motor system. *Appl Neurophysiol* 39: 222–238, 1976. doi:[10.1159/000102498](https://doi.org/10.1159/000102498).
15. Allen GI, Tsukahara N. Cerebrocerebellar communication systems. *Physiol Rev* 54: 957–1006, 1974. doi:[10.1152/physrev.1974.54.4.957](https://doi.org/10.1152/physrev.1974.54.4.957).
16. Rispal-Padel L, Cicirata F, Pons C. Contribution of the dentato-thalamo-cortical system to control of motor synergy. *Neurosci Lett* 22: 137–144, 1981. doi:[10.1016/0304-3940\(81\)90077-x](https://doi.org/10.1016/0304-3940(81)90077-x).
17. Babinski J. Asynergie et inertie cerebelleuses. *Rev Neurol* 14: 685–686, 1906.
18. Holmes G. The symptoms of acute cerebellar injuries due to gunshot injuries. *Brain* 40: 461–535, 1917. doi:[10.1093/brain/40.4.461](https://doi.org/10.1093/brain/40.4.461).
19. Holmes G. The cerebellum of man. *Brain* 62: 1–30, 1939. doi:[10.1093/brain/62.1.1](https://doi.org/10.1093/brain/62.1.1).
20. Chambers WW, Sprague JM. Functional localization in the cerebellum. II. Somatotopic organization in cortex and nuclei. *AMA Arch Neurol Psychiatry* 74: 653–680, 1955. doi:[10.1001/archneurpsyc.1955.02330180071008](https://doi.org/10.1001/archneurpsyc.1955.02330180071008).
21. Dow RS, Moruzzi G. *The Physiology and Pathology of the Cerebellum*. Minneapolis, MN: Minnesota University Press, 1958.
22. Arshavsky YI, Gelfand IM, Orlovsky GN. *Cerebellum and Rhythmic Movements*. Berlin: Springer, 1986.
23. Evarts EV. Activity of thalamic and cortical neurons in relation to learned movement in the monkey. *Int J Neurol* 8: 321–326, 1971.

24. Strick PL. Activity of ventrolateral thalamic neurons during arm movement. *J Neurophysiol* 39: 1032–1044, 1976. doi:[10.1152/jn.1976.39.5.1032](https://doi.org/10.1152/jn.1976.39.5.1032).

25. Neafsey EJ, Hull CD, Buchwald NA. Preparation for movement in the cat. II. Unit activity in the basal ganglia and thalamus. *Electroencephalogr Clin Neurophysiol* 44: 714–723, 1978. doi:[10.1016/0013-4694\(78\)90206-7](https://doi.org/10.1016/0013-4694(78)90206-7).

26. Schmied A, Benita M, Conde H, Dormont JF. Activity of ventrolateral thalamic neurons in relation to a simple reaction time task in the cat. *Exp Brain Res* 36: 285–300, 1979. doi:[10.1007/BF00238912](https://doi.org/10.1007/BF00238912).

27. van Donkelaar P, Stein JF, Passingham RE, Miall RC. Neuronal activity in the primate motor thalamus during visually triggered and internally generated limb movements. *J Neurophysiol* 82: 934–945, 1999. doi:[10.1152/jn.1999.82.2.934](https://doi.org/10.1152/jn.1999.82.2.934).

28. Kurata K. Activity properties and location of neurons in the motor thalamus that project to the cortical motor areas in monkeys. *J Neurophysiol* 94: 550–566, 2005. doi:[10.1152/jn.01034.2004](https://doi.org/10.1152/jn.01034.2004).

29. Marlinski V, Nilawera WU, Zelenin PV, Sirota MG, Beloozerova IN. Signals from the ventrolateral thalamus to the motor cortex during locomotion. *J Neurophysiol* 107: 455–472, 2012. doi:[10.1152/jn.0113.2010](https://doi.org/10.1152/jn.0113.2010).

30. Orlovsky GN, Deliagina TG, Grillner S. Neuronal Control of Locomotion. From Mollusc to Man. New York: Oxford University Press, 1999.

31. Glickstein M. How are visual areas of the brain connected to motor areas for the sensory guidance of movement? *Trends Neurosci* 23: 613–617, 2000. doi:[10.1016/s0166-2236\(00\)01681-7](https://doi.org/10.1016/s0166-2236(00)01681-7).

32. Trendelenburg W. Untersuchungen über reizlose vorübergehende Aussaltung am Zentralnervensystem. III. Die extirpata Region der Grosshirnrinde. *Pflüger's Arch* 137: 515–544, 1911. doi:[10.1007/BF01680423](https://doi.org/10.1007/BF01680423).

33. Liddell EGT, Phillips CG. Pyramidal section in the cat. *Brain* 67: 1–9, 1944. doi:[10.1093/brain/67.1.1](https://doi.org/10.1093/brain/67.1.1).

34. Beloozerova IN, Sirota MG. The role of the motor cortex in the control of accuracy of locomotor movements in the cat. *J Physiol* 461: 1–25, 1993. doi:[10.1113/jphysiol.1993.sp019498](https://doi.org/10.1113/jphysiol.1993.sp019498).

35. Metz GA, Whishaw IQ. Cortical and subcortical lesions impair skilled walking in the ladder rung walking test: a new task to evaluate fore- and hindlimb stepping, placing, and co-ordination. *J Neurosci Methods* 115: 169–179, 2002. doi:[10.1016/s0165-0270\(02\)00012-2](https://doi.org/10.1016/s0165-0270(02)00012-2).

36. Den Otter AR, Geurts AC, de Haart M, Mulder T, Duysens J. Step characteristics during obstacle avoidance in hemiplegic stroke. *Exp Brain Res* 161: 180–192, 2005. doi:[10.1007/s00221-004-2057-0](https://doi.org/10.1007/s00221-004-2057-0).

37. Farr TD, Liu L, Colwell KL, Whishaw IQ, Metz GA. Bilateral alteration in stepping pattern after unilateral motor cortex injury: a new test strategy for analysis of skilled limb movements in neurological mouse models. *J Neurosci Methods* 153: 104–113, 2006. doi:[10.1016/j.jneumeth.2005.10.011](https://doi.org/10.1016/j.jneumeth.2005.10.011).

38. Friel KM, Drew T, Martin JH. Differential activity-dependent development of corticospinal control of movement and final limb position during visually guided locomotion. *J Neurophysiol* 97: 3396–3406, 2007. doi:[10.1152/jn.00750.2006](https://doi.org/10.1152/jn.00750.2006).

39. Asante CO, Chu A, Fisher M, Benson L, Beg A, Scheiffele P, Martin J. Cortical control of adaptive locomotion in wild-type mice and mutant mice lacking the ephrin-Eph effector protein alpha2-chimaerin. *J Neurophysiol* 104: 3189–3202, 2010. doi:[10.1152/jn.00671.2010](https://doi.org/10.1152/jn.00671.2010).

40. Armstrong DM, Drew T. Discharges of pyramidal tract and other motor cortical neurons during locomotion in the cat. *J Physiol* 346: 471–495, 1984. doi:[10.1113/jphysiol.1984.sp015036](https://doi.org/10.1113/jphysiol.1984.sp015036).

41. Armstrong DM, Drew T. Locomotor-related neuronal discharges in cat motor cortex compared with peripheral receptive fields and evoked movements. *J Physiol* 346: 497–517, 1984. doi:[10.1113/jphysiol.1984.sp015037](https://doi.org/10.1113/jphysiol.1984.sp015037).

42. Beloozerova IN, Sirota MG. Activity of neurons of the motosensory cortex during natural locomotion in the cat. *Neurofisiologia* 17: 406–408, 1985.

43. Beloozerova IN, Sirota MG. The role of the motor cortex in the control of vigour of locomotor movements in the cat. *J Physiol* 461: 27–46, 1993. doi:[10.1113/jphysiol.1993.sp019499](https://doi.org/10.1113/jphysiol.1993.sp019499).

44. Drew T. Motor cortical cell discharge during voluntary gait modification. *Brain Res* 457: 181–187, 1988. doi:[10.1016/0006-8993\(88\)90073-x](https://doi.org/10.1016/0006-8993(88)90073-x).

45. Drew T. Motor cortical activity during voluntary gait modifications in the cat. I. Cells related to the forelimbs. *J Neurophysiol* 70: 179–199, 1993. doi:[10.1152/jn.1993.70.1.179](https://doi.org/10.1152/jn.1993.70.1.179).

46. Widajewicz W, Kably B, Drew T. Motor cortical activity during voluntary gait modifications in the cat. II. Cells related to the hindlimbs. *J Neurophysiol* 72: 2070–2089, 1994. doi:[10.1152/jn.1994.72.5.2070](https://doi.org/10.1152/jn.1994.72.5.2070).

47. Fitzsimmons NA, Lebedev MA, Peikon ID, Nicolelis MA. Extracting kinematic parameters for monkey bipedal walking from cortical neuronal ensemble activity. *Frontiers in Integrative Neurosci* 3: 3, 2009. doi:[10.3389/neuro.07.003.2009](https://doi.org/10.3389/neuro.07.003.2009).

48. Gwin JT, Gramann K, Makeig S, Ferris DP. Electrocortical activity is coupled to gait cycle phase during treadmill walking. *Neuroimage* 54: 1289–1296, 2011. doi:[10.1016/j.neuroimage.2010.08.066](https://doi.org/10.1016/j.neuroimage.2010.08.066).

49. Stout EE, Beloozerova IN. Pyramidal tract neurons receptive to different forelimb joints act differently during locomotion. *J Neurophysiol* 107: 1890–1903, 2012. doi:[10.1152/jn.00650.2011](https://doi.org/10.1152/jn.00650.2011).

50. Stout EE, Beloozerova IN. Differential responses of fast- and slow-conducting pyramidal tract neurons to changes in accuracy demands during locomotion. *J Physiol* 591: 2647–2666, 2013. doi:[10.1113/jphysiol.2012.232538](https://doi.org/10.1113/jphysiol.2012.232538).

51. Farrell BJ, Bulgakova MA, Beloozerova IN, Sirota MG, Prilutsky BI. Body stability and muscle and motor cortex activity during walking with wide stance. *J Neurophysiol* 112: 504–524, 2014. doi:[10.1152/jn.00064.2014](https://doi.org/10.1152/jn.00064.2014).

52. Farrell BJ, Bulgakova MA, Sirota MG, Prilutsky BI, Beloozerova IN. Accurate stepping on a narrow path: mechanics, EMG, and motor cortex activity in the cat. *J Neurophysiol* 114: 2682–2702, 2015. doi:[10.1152/jn.00510.2014](https://doi.org/10.1152/jn.00510.2014).

53. Stout EE, Sirota MG, Beloozerova IN. Known and unexpected constraints evoke different kinematic, muscle, and motor cortical neuron responses during locomotion. *Eur J Neurosci* 42: 2666–2677, 2015. doi:[10.1111/ejn.13053](https://doi.org/10.1111/ejn.13053).

54. Seeber M, Scherer R, Wagner J, Solis-Escalante T, Möller-Putz GR. High and low gamma EEG oscillations in central sensorimotor areas are conversely modulated during the human gait cycle. *Neuroimage* 112: 318–326, 2015. doi:[10.1016/j.neuroimage.2015.03.045](https://doi.org/10.1016/j.neuroimage.2015.03.045).

55. Wagner J, Makeig S, Gola M, Neuper C, Möller-Putz G. Distinct? Band oscillatory networks subserving motor and cognitive control during gait adaptation. *J Neurosci* 36: 2212–2226, 2016. doi:[10.1523/JNEUROSCI.3543-15.2016](https://doi.org/10.1523/JNEUROSCI.3543-15.2016).

56. DiGiovanna J, Dominici N, Friedli L, Rigosa J, Duis S, Kreider J, Beauparlant J, van den Brand R, Schieppati M, Micera S, Courtine G. Engagement of the rat hindlimb motor cortex across natural locomotor behaviors. *J Neurosci* 36: 10440–10455, 2016. doi:[10.1523/JNEUROSCI.4343-15.2016](https://doi.org/10.1523/JNEUROSCI.4343-15.2016).

57. Bradford JC, Lukos JR, Ferris DP. Electrocortical activity distinguishes between uphill and level walking in humans. *J Neurophysiol* 115: 958–966, 2016. doi:[10.1152/jn.00089.2015](https://doi.org/10.1152/jn.00089.2015).

58. Miri A, Warriner CL, Seely JS, Elsayed GF, Cunningham JP, Churchland MM, Jessell TM. Behaviorally selective engagement of short-latency effector pathways by motor cortex. *Neuron* 95: 683–696.e11, 2017. doi:[10.1016/j.neuron.2017.06.042](https://doi.org/10.1016/j.neuron.2017.06.042).

59. Xing D, Aghagolzadeh M, Truccolo W, Borton D. Low-dimensional motor cortex dynamics preserve kinematics information during unconstrained locomotion in nonhuman primates. *Front Neurosci* 13: 1046, 2019. doi:[10.3389/fnins.2019.01046](https://doi.org/10.3389/fnins.2019.01046). eCollection 2019.

60. Nordin AD, Hairston WD, Ferris DP. Human electrocortical dynamics while stepping over obstacles. *Sci Rep* 9: 4693, 2019. doi:[10.1038/s41598-019-4113-2](https://doi.org/10.1038/s41598-019-4113-2).

61. Yokoyama H, Kaneko N, Masugi Y, Ogawa T, Watanabe K, Nakazawa K. Gait-phase-dependent and gait-phase-independent cortical activity across multiple regions involved in voluntary gait modifications in humans. *Eur J Neurosci* 00: 1–14, 2020. doi:[10.1111/ejn.14867](https://doi.org/10.1111/ejn.14867).

62. Baron JC, D'Antona R, Pantano P, Serdar M, Samson Y, Bousser MG. Effects of thalamic stroke on energy metabolism of the cerebral cortex. A positron tomography study in man. *Brain* 109: 1243–1259, 1986. doi:[10.1093/brain/109.6.1243](https://doi.org/10.1093/brain/109.6.1243).

63. Baron JC, Levasseur M, Mazoyer B, Legault-Demare F, Mauguire F, Pappata S, Jedynak P, Derome P, Cambier J, Tran-Dinh S. Thalamocortical diaschisis: positron emission tomography in humans. *J Neurol Neurosurg Psychiatry* 55: 935–942, 1992. doi:[10.1136/jnnp.55.10.935](https://doi.org/10.1136/jnnp.55.10.935).

64. Lewis DH, Toney LK, Baron JC. Nuclear medicine in cerebrovascular disease. *Semin Nucl Med* 42: 387–405, 2012. doi:[10.1053/j.semnuclmed.2012.06.002](https://doi.org/10.1053/j.semnuclmed.2012.06.002).

65. Ward NS, Brown MM, Thompson AJ, Frackowiak RSJ. Neural correlates of outcome after stroke: a cross-sectional fMRI study. *Brain* 126: 1430–1448, 2003. doi:[10.1093/brain/awg145](https://doi.org/10.1093/brain/awg145).

66. Favre I, Zeffiro TA, Detante O, Krainik A, Hommel M, Jaillard A. Upper limb recovery after stroke is associated with ipsilesional primary motor cortical activity: a meta-analysis. *Stroke* 45: 1077–1083, 2014. doi:[10.1161/STROKEAHA.113.003168](https://doi.org/10.1161/STROKEAHA.113.003168).

67. Baron JC. Clinical use of positron emission tomography in cerebrovascular diseases. *Neurosurg Clin N Am* 7: 653–664, 1996.

68. Cirstea CM, Brooks WM, Craciunas SC, Popescu EA, Choi IY, Lee P, Bani-Ahmed A, Yeh HW, Savage CR, Cohen LG, Nudo RJ. Primary motor cortex in stroke: a functional MRI-guided proton MR spectroscopic study. *Stroke* 42: 1004–1009, 2011. doi:[10.1161/STROKEAHA.110.601047](https://doi.org/10.1161/STROKEAHA.110.601047).

69. Bundy DT, Nudo RJ. Preclinical studies of neuroplasticity following experimental brain injury. *Stroke* 50: 2626–2633, 2019. doi:[10.1161/STROKEAHA.119.023550](https://doi.org/10.1161/STROKEAHA.119.023550).

70. Cassidy JM, Wodeyar A, Wu J, Kaur K, Masuda AK, Srinivasan R, Cramer SC. Low-frequency oscillations are a biomarker of injury and recovery after stroke. *Stroke* 51: 1442–1450, 2020. doi:[10.1161/STROKEAHA.120.028932](https://doi.org/10.1161/STROKEAHA.120.028932).

71. Ichikawa M, Arissian K, Asanuma H. Reorganization of the projection from the sensory cortex to the motor cortex following elimination of the thalamic projection to the motor cortex in cats; Golgi, electron microscope and degeneration study. *Brain Res* 437: 131–141, 1987. doi:[10.1016/0006-8993\(87\)91534-4](https://doi.org/10.1016/0006-8993(87)91534-4).

72. Chernyshevskaya IA, Sidorov BM. [Compensatory processes in the motor cortex of the cerebral hemispheres in partial damage to the ventrolateral thalamic nucleus in the cat]. *Zh Vyssh Nerv Deiat Im I P Pavlova* 41: 1050–1058, 1991.

73. Asanuma H, Kosar E, Tsukahara N, Robinson H. Modification of the projection from the sensory cortex to the motor cortex following the elimination of thalamic projections to the motor cortex in cats. *Brain Res* 345: 79–86, 1985. doi:[10.1016/0006-8993\(85\)90838-8](https://doi.org/10.1016/0006-8993(85)90838-8).

74. Chen R, Cohen LG, Hallett M. Nervous system reorganization following injury. *Neuroscience* 111: 761–773, 2002. doi:[10.1016/s0306-4522\(02\)00025-8](https://doi.org/10.1016/s0306-4522(02)00025-8).

75. Cramer SC. Repairing the human brain after stroke. I. Mechanisms of spontaneous recovery. *Ann Neurol* 63: 272–287, 2008. doi:[10.1002/ana.21393](https://doi.org/10.1002/ana.21393).

76. Calautti C, Baron JC. Functional neuroimaging studies of motor recovery after stroke in adults: a review. *Stroke* 34: 1553–1566, 2003. doi:[10.1161/01.STR.0000071761.36075.A6](https://doi.org/10.1161/01.STR.0000071761.36075.A6).

77. Sidorov BM. Long-term ongoing reorganizations of the processes of analysis of kinesthetic afferentation at the level of cat motor cortex neurons after damage to the ventrolateral nucleus of the thalamus. *Neurosci Behav Physiol* 25: 488–496, 1995. doi:[10.1007/BF02359277](https://doi.org/10.1007/BF02359277).

78. Beloozerova IN, Marlinski V. Contribution of the ventrolateral thalamus to the locomotion-related activity of motor cortex. *J Neurophysiol* 124: 1480–1504, 2020. doi:[10.1152/jn.00253.2020](https://doi.org/10.1152/jn.00253.2020).

79. Armstrong DM, Drew T. Topographical localization in the motor cortex of the cat for somatic afferent responses and evoked movements. *J Physiol* 350: 33–54, 1984. doi:[10.1113/jphysiol.1984.sp015187](https://doi.org/10.1113/jphysiol.1984.sp015187).

80. Beloozerova IN, Farrell BJ, Sirota MG, Prilutsky BI. Differences in movement mechanics, electromyographic, and motor cortex activity between accurate and non-accurate stepping. *J Neurophysiol* 103: 2285–2300, 2010. doi:[10.1152/jn.00360.2009](https://doi.org/10.1152/jn.00360.2009).

81. Armer MC, Nilawera WU, Rivers TJ, Dasgupta NM, Beloozerova IN. Effect of light on the activity of motor cortex during locomotion. *Behav Brain Res* 250: 238–250, 2013. doi:[10.1016/j.bbr.2013.05.004](https://doi.org/10.1016/j.bbr.2013.05.004).

82. Honore T, Davies SN, Drejer J, Fletcher EJ, Jacobsen P, Lodge D, Nielsen FE. Quinoxalinediones: potent competitive non-NMDA glutamate receptor antagonists. *Science* 241: 701–703, 1988. doi:[10.1126/science.2899909](https://doi.org/10.1126/science.2899909).

83. Lee SH, Govindaraj G, Cox CL. Selective excitatory actions of DNXQ and CNQX in rat thalamic neurons. *J Neurophysiol* 103: 1728–1734, 2010. doi:[10.1152/jn.00540.2009](https://doi.org/10.1152/jn.00540.2009).

84. Coyle JT, Molliver ME, Kuhar MJ. In situ injection of kainic acid: A new method for selectively lesioning neuronal cell bodies while sparing axons of passage. *J Comp Neurol* 180: 301–323, 1978. doi:[10.1002/cne.901800208](https://doi.org/10.1002/cne.901800208).

85. Sherk H. Functional organization of input from areas 17 and 18 to an extrastriate area in the cat. *J Neurosci* 10: 2780–2790, 1990. doi:[10.1523/JNEUROSCI.10-08-02780.1990](https://doi.org/10.1523/JNEUROSCI.10-08-02780.1990).

86. Asanuma H, Stoney SD Jr, Abzug C. Relationship between afferent input and motor outflow in cat motosensory cortex. *J Neurophysiol* 31: 670–681, 1968. doi:[10.1152/jn.1968.31.5.670](https://doi.org/10.1152/jn.1968.31.5.670).

87. Murphy JT, Wong YC, Kwan HC. Afferent-efferent linkages in motor cortex for single forelimb muscles. *J Neurophysiol* 38: 990–1014, 1975. doi:[10.1152/jn.1975.38.4.990](https://doi.org/10.1152/jn.1975.38.4.990).

88. Rosen I, Asanuma H. Peripheral afferent input to the forelimb area of the monkey motor cortex: input-output relations. *Exp Brain Res* 14: 257–273, 1972. doi:[10.1007/BF00816162](https://doi.org/10.1007/BF00816162).

89. Sakata H, Miyamoto J. Topographic relationship between the receptive fields of neurons in the motor cortex and the movements elicited by focal stimulation in freely moving cats. *Jpn J Physiol* 18: 489–507, 1968. doi:[10.2170/jjphysiol.18.489](https://doi.org/10.2170/jjphysiol.18.489).

90. Prilutsky BI, Sirota MG, Gregor RJ, Beloozerova IN. Quantification of motor cortex activity and full-body biomechanics during unconstrained locomotion. *J Neurophysiol* 94: 2959–2969, 2005. doi:[10.1152/jn.00704.2004](https://doi.org/10.1152/jn.00704.2004).

91. Chambers WWV, Liu CN. Corticospinal tract of the cat. An attempt to correlate the pattern of degeneration with deficit in reflex act following neocortical lesions. *J Comp Neurol* 108: 23–26, 1957. doi:[10.1002/cne.901080103](https://doi.org/10.1002/cne.901080103).

92. Skinner BF. The Behavior of Organisms. New York: Appleton-Century-Crofts Inc., 1938.

93. Pryor K. Lads Before the Wind. New York: Harper and Row, 1975.

94. de Carvalho WD, Rosalino LM, Dalponte JC, Santos B, Harumi Adania C, Lustosa Esberard CE. Can footprints of small and medium sized felids be distinguished in the field? Evidences from Brazil's Atlantic Forest. *Trop Conserv Sci* 8: 760–777, 2015. doi:[10.14008291500800313](https://doi.org/10.14008291500800313).

95. Zelenin PV, Beloozerova IN, Sirota MG, Orlovsky GN, Deliagina TG. Activity of red nucleus neurons in the cat during postural corrections. *J Neurosci* 30: 14533–14542, 2010. doi:[10.1523/JNEUROSCI.2991-10.2010](https://doi.org/10.1523/JNEUROSCI.2991-10.2010).

96. Nieoullon A, Rispal-Padel L. Somatotopic localization in cat motor cortex. *Brain Res* 105: 405–422, 1976. doi:[10.1016/0006-8993\(76\)90590-4](https://doi.org/10.1016/0006-8993(76)90590-4).

97. Phillips CG, Porter R. Corticospinal neurons. Their role in movement. *Monogr Physiol Soc* 34: v–xii, 1–450, 1977.

98. Vicario DS, Martin JH, Ghez C. Specialized subregions in the cat motor cortex: a single unit analysis in the behaving animal. *Exp Brain Res* 51: 351–367, 1983. doi:[10.1007/BF00237872](https://doi.org/10.1007/BF00237872).

99. Armstrong DM, Drew T. Electromyographic responses evoked in muscles of the forelimb by intracortical stimulation in the cat. *J Physiol* 367: 309–326, 1985. doi:[10.1113/jphysiol.1985.sp015826](https://doi.org/10.1113/jphysiol.1985.sp015826).

100. Martin JH, Ghez C. Differential impairments in reaching and grasping produced by local inactivation within the forelimb representation of the motor cortex in the cat. *Exp Brain Res* 94: 429–443, 1993. doi:[10.1007/BF00230201](https://doi.org/10.1007/BF00230201).

101. Bishop PO, Burke W, Davis R. The identification of single units in central visual pathways. *J Physiol* 162: 409–431, 1962. doi:[10.1113/jphysiol.1962.sp006942](https://doi.org/10.1113/jphysiol.1962.sp006942).

102. Fuller JH, Schlag J. Determination of antidromic excitation by the collision test: problems of interpretation. *Brain Res* 112: 283–298, 1976. doi:[10.1016/0006-8993\(76\)90284-5](https://doi.org/10.1016/0006-8993(76)90284-5).

103. Takahashi K. Slow and fast groups of pyramidal tract cells and their respective membrane properties. *J Neurophysiol* 28: 908–924, 1965. doi:[10.1152/jn.1965.28.5.908](https://doi.org/10.1152/jn.1965.28.5.908).

104. Reinoso-Suarez F. Topographischer Hirnatlas der Katze für Experimental-Physiologische Untersuchungen. Darmstadt, Germany: E. Merck AG, 1961.

105. Nieoullon A, Kerkerian L, Dusticier N. High affinity glutamate uptake in the red nucleus and ventrolateral thalamus after lesion of the cerebellum in the adult cat: biochemical evidence for functional changes in the deafferented structures. *Exp Brain Res* 55: 409–419, 1984. doi:[10.1007/BF00235271](https://doi.org/10.1007/BF00235271).

106. Kerkerian L, Nieoullon A, Dusticier N. Brain glutamate uptake: regional distribution study from sensorimotor areas in the cat. *Neurochem Int* 4: 275–281, 1982. doi:[10.1016/0197-0186\(82\)90064-x](https://doi.org/10.1016/0197-0186(82)90064-x).

107. Broman J, Ottersen OP. Cervicothalamic tract terminals are enriched in glutamate-like immunoreactivity: an electron microscopic double-labeling study in the cat. *J Neurosci* 12: 204–221, 1992. doi:[10.1523/JNEUROSCI.12-01-00204.1992](https://doi.org/10.1523/JNEUROSCI.12-01-00204.1992).

108. Ericson AC, Blomqvist A, Craig AD, Ottersen OP, Broman J. Evidence for glutamate as neurotransmitter in trigemino-and spinothalamic tract terminals in the nucleus submedius of cats. *Eur J Neurosci* 7: 305–317, 1995. doi:[10.1111/j.1460-9568.1995.tb01066.x](https://doi.org/10.1111/j.1460-9568.1995.tb01066.x).

109. Myers RD. Injection of solutions into cerebral tissue: relation between volume and diffusion. *Physiol Behav* 1: 171–174, 1966. doi:[10.1016/0031-9384\(66\)90064-3](https://doi.org/10.1016/0031-9384(66)90064-3).

110. Efron B, Tibshirani RJ. An Introduction to the Bootstrap. New York: Chapman & Hall, 1993.

111. Batschelet E. Circular Statistics in Biology. London: Academic Press, 1981.

112. Drew T, Doucet S. Application of circular statistics to the study of neuronal discharge during locomotion. *J Neurosci Methods* 38: 171–181, 1991. doi:[10.1016/0165-0270\(91\)90167-X](https://doi.org/10.1016/0165-0270(91)90167-X).

113. Fischer NI. Statistical Analysis of Circular Data. Cambridge, UK: Cambridge University Press, 1993.

114. Shik ML, Orlovsky GN. Neurophysiology of locomotor automatism. *Physiol Rev* 56: 465–501, 1976. doi:[10.1152/physrev.1976.56.3.465](https://doi.org/10.1152/physrev.1976.56.3.465).

115. Grillner S, Zanger P. On the central generation of locomotion in the low spinal cat. *Exp Brain Res* 34: 241–261, 1979. doi:[10.1007/BF00235671](https://doi.org/10.1007/BF00235671).

116. Forssberg H, Grillner S, Halbertsma J. The locomotion of the low spinal cat. I. Coordination within a hindlimb. *Acta Physiol Scand* 108: 269–281, 1980. doi:[10.1111/j.1748-1716.1980.tb06533.x](https://doi.org/10.1111/j.1748-1716.1980.tb06533.x).

117. Forssberg H, Grillner S, Halbertsma J, Rossignol S. The locomotion of the low spinal cat. II. Interlimb coordination. *Acta Physiol Scand* 108: 283–295, 1980. doi:[10.1111/j.1748-1716.1980.tb06534.x](https://doi.org/10.1111/j.1748-1716.1980.tb06534.x).

118. Magnus R. Körperstellung. Berlin: Springer, 1924.

119. Bard P, Macht MB. The behavior of chronically decerebrate cat. In: *Neurological Basis of Behavior*, edited by Wolstenholme GEW, O'Connor CM. London: Churchill, 1958, p. 55–71.

120. Deliagina TG, Beloozerova IN, Zelenin PV, Orlovsky GN. Spinal and supraspinal postural networks. *Brain Res Rev* 57: 212–221, 2008. doi:[10.1016/j.brainresrev.2007.06.017](https://doi.org/10.1016/j.brainresrev.2007.06.017).

121. Deliagina TG, Beloozerova IN, Orlovsky GN, Zelenin PV. Contribution of supraspinal systems to generation of automatic postural responses. *Front Integr Neurosci* 8: 76, 2014. doi:[10.3389/fnint.2014.00076](https://doi.org/10.3389/fnint.2014.00076). eCollection 2014.

122. Matthijs JS, Barton SL, Fajen BR. The critical phase for visual control of human walking over complex terrain. *Proc Natl Acad Sci USA* 114: E6720–E6729, 2017. doi:[10.1073/pnas.1611699114](https://doi.org/10.1073/pnas.1611699114).

123. Matthijs JS, Yates JL, Hayhoe MM. Gaze and the control of foot placement when walking in natural terrain. *Curr Biol* 28: 1224–1233. e5, 2018. doi:[10.1016/j.cub.2018.03.008](https://doi.org/10.1016/j.cub.2018.03.008).

124. Zubair HN, Chu KML, Johnson JL, Rivers TJ, Beloozerova IN. Gaze coordination with strides during walking in the cat. *J Physiol* 597: 5195–5229, 2019. doi:[10.1113/JP278108](https://doi.org/10.1113/JP278108).

125. Drew T, Andujar JE, Lajoie K, Yakovenko S. Cortical mechanisms involved in visuomotor coordination during precision walking. *Brain Res Rev* 57: 199–211, 2008. doi:[10.1016/j.brainresrev.2007.07.017](https://doi.org/10.1016/j.brainresrev.2007.07.017).

126. Shinoda Y, Kakei S, Futami T, Wannier T. Thalamocortical organization in the cerebello-thalamo-cortical system. *Cereb Cortex* 3: 421–429, 1993. doi:[10.1093/cercor/3.5.421](https://doi.org/10.1093/cercor/3.5.421).

127. Rivers TJ, Sirota MG, Guttentag AI, Ogorodnikov DA, Shah NA, Beloozerova IN. Gaze shifts and fixations dominate gaze behavior of walking cats. *Neuroscience* 275: 477–499, 2014. doi:[10.1016/j.neuroscience.2014.06.034](https://doi.org/10.1016/j.neuroscience.2014.06.034).

128. Klishko AN, Farrell BJ, Beloozerova IN, Latash ML, Prilutsky BI. Stabilization of cat paw trajectory during locomotion. *J Neurophysiol* 112: 1376–1391, 2014. doi:[10.1152/jn.00663.2013](https://doi.org/10.1152/jn.00663.2013).

129. Hollands MA, Marple-Horvat DE. Visually guided stepping under conditions of step cycle-related denial of visual information. *Exp Brain Res* 109: 343–356, 1996. doi:[10.1007/BF00231792](https://doi.org/10.1007/BF00231792).

130. Kawai R, Markman T, Poddar R, Ko R, Fantana AL, Dhawale AK, Kampff AR, Ölveczky BP. Motor cortex is required for learning but not for executing a motor skill. *Neuron* 86: 800–812, 2015. doi:[10.1016/j.neuron.2015.03.024](https://doi.org/10.1016/j.neuron.2015.03.024).

131. Zubair HN, Stout EE, Dounskoia N, Beloozerova IN. The role of inter-segmental dynamics in coordination of the forelimb joints during unperturbed and perturbed skilled locomotion. *J Neurophysiol* 120: 1547–1557, 2018. doi:[10.1152/jn.00324.2018](https://doi.org/10.1152/jn.00324.2018).

132. von Monakow C. Die Localization im Grosshirn und der Abbau der Funktion durch korticale Herde. Wiesbaden, Germany: JF Bergmann, 1914.

133. Feeney DM, Baron JC. Diaschisis. *Stroke* 17: 817–830, 1986. doi:[10.1161/01.str.17.5.817](https://doi.org/10.1161/01.str.17.5.817).

134. Carrera E, Tononi G. Diaschisis: past, present, future. *Brain* 137: 2408–2422, 2014. doi:[10.1093/brain/awu101](https://doi.org/10.1093/brain/awu101).

135. Berman AL, Jones EG. The Thalamus and Basal Telencephalon of the Cat: A Cytoarchitectonic Atlas with Stereotaxic Coordinates. Madison, WI: University of Wisconsin Press, 1982.